REPORT NO. NADC-90004-60

AD-A233 654

A MODEL FOR THE THERMOPLASTIC ANALYSIS OF METAL MATRIX LAMINATES

David J. Barrett
Air Vehicle and Crew Systems Technology Department (Code 6043)
NAVAL AIR DEVELOPMENT CENTER
Warminster, PA 18974-5000

20 DECEMBER 1989

PROGRESS REPORT
Period Covering August 1989 to December 1989
Task No. A9329-32J
Work Unit No. KG 990
Program Element No. 63269F

DTIC
ELECTE
APR 10 1991
S B D

Approved for Public Release; Distribution is Unlimited

Prepared for
NAVAL AIR SYSTEM COMMAND
Department of the Navy
Washington, DC 20361-0001

DTIC FILE COPY

91 4 09 024

NOTICES

REPORT NUMBERING SYSTEM — The numbering of technical project reports issued by the Naval Air Development Center is arranged for specific identification purposes. Each number consists of the Center acronym, the calendar year in which the number was assigned, the sequence number of the report within the specific calendar year, and the official 2-digit correspondence code of the Command Officer or the Functional Department responsible for the report. For example: Report No. NADC-88020-60 indicates the twentieth Center report for the year 1988 and prepared by the Air Vehicle and Crew Systems Technology Department. The numerical codes are as follows:

CODE	OFFICE OR DEPARTMENT
00	Commander, Naval Air Development Center
01	Technical Director, Naval Air Development Center
05	Computer Department
10	AntiSubmarine Warfare Systems Department
20	Tactical Air Systems Department
30	Warfare Systems Analysis Department
40	Communication Navigation Technology Department
50	Mission Avionics Technology Department
60	Air Vehicle & Crew Systems Technology Department
70	Systems & Software Technology Department
80	Engineering Support Group
90	Test & Evaluation Group

PRODUCT ENDORSEMENT — The discussion or instructions concerning commercial products herein do not constitute an endorsement by the Government nor do they convey or imply the license or right to use such products.

Reviewed By: ____________________ Date: 7/25/90
Branch Head

Reviewed By: ____________________ Date: 7/27/90
Division Head

Reviewed By: ____________________ Date: 1 Aug 90
Director/Deputy Director

REPORT DOCUMENTATION PAGE

Form Approved
OMB No 0704-0188

1a REPORT SECURITY CLASSIFICATION Unclassified	1b RESTRICTIVE MARKINGS
2a SECURITY CLASSIFICATION AUTHORITY	3 DISTRIBUTION/AVAILABILITY OF REPORT Approved for public release; distribution is unlimited.
2b DECLASSIFICATION/DOWNGRADING SCHEDULE	
4 PERFORMING ORGANIZATION REPORT NUMBER(S) NADC-90004-60	5 MONITORING ORGANIZATION REPORT NUMBER(S)
6a NAME OF PERFORMING ORGANIZATION Air Vehicle and Crew Systems Technology Department 6b OFFICE SYMBOL (If applicable) 6043	7a NAME OF MONITORING ORGANIZATION
6c. ADDRESS (City, State, and ZIP Code) NAVAL AIR DEVELOPMENT CENTER Warminster, PA 18974-5000	7b ADDRESS (City, State, and ZIP Code)
8a. NAME OF FUNDING/SPONSORING ORGANIZATION NAVAL AIR SYSTEMS COMMAND 8b OFFICE SYMBOL (If applicable) AIR-931B	9 PROCUREMENT INSTRUMENT IDENTIFICATION NUMBER
8c. ADDRESS (City, State, and ZIP Code) Washington, DC 20361-0001	10 SOURCE OF FUNDING NUMBERS PROGRAM ELEMENT NO 63269F · PROJECT NO 0 · TASK NO A9329 32J · WORK UNIT ACCESSION NO KG 990

11 TITLE (Include Security Classification)
A Model For The Thermoplastic Analysis Of Metal Matrix Laminates

12 PERSONAL AUTHOR(S)
David Jonn Barrett

13a TYPE OF REPORT	13b TIME COVERED	14 DATE OF REPORT (Year, Month, Day)	15 PAGE COUNT
Progress	FROM 8/89 TO 12/89	1989 December 20	

16 SUPPLEMENTARY NOTATION

17 COSATI CODES

FIELD	GROUP	SUB-GROUP
11	04	
20	11	

18 SUBJECT TERMS (Continue on reverse if necessary and identify by block number)
Metal Matrix Composites, Thermoplasticity, Hot Structures

19 ABSTRACT (Continue on reverse if necessary and identify by block number)

This report describes the development of a theoretical model for the thermoplastic analysis of metal matrix fiber reinforced laminates. The nonlinear analysis is based on an incremental form of classical lamination theory in which the laminate can be loaded by residual stresses, thermal loads and edge stress resultants. The constituent stresses of the layers of the laminate are computed as the phase average stresses of the Composite Cylinder Assemblage. The matrix plasticity is treated by a transversely isotropic J_2 theory with the exception that the response is found in an average sense since the onset of plastic flow (von Mises' yield surface) and the flow itself (Prager's Rule) are based on the matrix phase average stresses. The hardening is temperature-dependent and kinematic. The mathematical model also accounts for the temperature dependency of the fiber and matrix material properties.

20 DISTRIBUTION/AVAILABILITY OF ABSTRACT ☐ UNCLASSIFIED/UNLIMITED ☒ SAME AS RPT ☐ DTIC USERS	21 ABSTRACT SECURITY CLASSIFICATION Unclassified
22a NAME OF RESPONSIBLE INDIVIDUAL David Jonn Barrett	22b TELEPHONE (Include Area Code) (215) 441-3770 · 22c OFFICE SYMBOL Code 6043

DD Form 1473, JUN 86 (Reverse)

CONTENTS

Accession For	
NTIS GRA&I	☑
DTIC TAB	☐
Unannounced	☐
Justification	
By	
Distribution/	
Availability Codes	
Dist	Avail and/or Special
A-1	

FIGURES

TABLES

SYMBOLS

Symbol	Definition
A	Laminate membrane stiffness matrix
B	Laminate membrane-bending stiffness matrix
D	Laminate bending stiffness matrix
E	Young's modulus
E_{TAN}	Tangential modulus
f_1, f_2	Functions representing the mathematical operations of the Composite Cylinder Assemblage model
g_1, g_2	Functions corresponding to the transversely isotropic approximation
h	Hardening parameter
k	Strength parameter
K	Matrix of plate curvatures
K_{xx}, K_{yy}, K_{xy}	Normal and twisting plate curvatures
M_{xx}, M_{yy}, M_{xy}	Normal and twisting plate moments
N_{xx}, N_{yy}, N_{xy}	Normal and shear stress resultants
Q	Layer stiffness matrix expressed in local coordinates
$\overline{Q}$	Layer compliance matrix expressed in gloobal coordinates
s	Layer compliance matrix expressed in local coodinates
S_{ij}	Matrix deviatoric stress tensor
S_{ijkl}	Compliance tensor
t	Plate thickness
T	Temperature
T_0	Reference temperature
u_x, u_y, u_z	Plate displacements
u_x^o, u_y^o, u_z^o	Reference surface displacements
V_f, V_m	Fiber and matrix volume fractions
x, y, z	Global coordinates
α_{ij}	Secant thermal expansivity
β	Thermal expansion matrix

Symbol	Definition
β_{ij}	Equivalent thermal expansion tensor
Γ	Thermal stress vector expressed in local coordinates
$\overline{\Gamma}$	Thermal stress vector expressed in global coordinates
γ_{xy}	Shear plate strain, engineering
γ°_{xy}	Midsurface shear strain, engineering
ϵ_1	Matrix of local ply strains
ϵ_x	Matrix of global laminate strains
ϵ_{xx}, ϵ_{yy}	Normal plate strains
ϵ^{o}_{xx}, ϵ^{o}_{yy},	Midsurface normal plate strains
ε°,	Matrix of midsurface plate strains
ϵ_{ij}	Strain tensor
θ	Ply orientation with respect to the global x coordinate
Θ_{ϵ}	Strain transformation matrix
Θ_{σ}	Stress transformation matrix
σ_1	Stress matrix
σ_y	Yield stress
σ_{ij}	Stress tensor
ϕ	Yield function
Ψ	Load function

Superscripts

E	An elastic quantity
F	A fiber quantity
M	A matrix quantity
P	A plastic quantity
T	A total quantity (elastic plus plastic components)
.	A rate quantity
–	Refers to the transversely isotropic approximation
–1	An inverse

INTRODUCTION

PURPOSE

This report describes the development of a thermoplasticity model for the analytical investigation of the behavior of metal matrix fiber reinforced laminates. The nonlinear analysis is based on an incremental form of classical lamination theory in which the laminate can be loaded by residual stresses, thermal loads, and edge stress resultants. The constituent stresses of the layers of the laminate are computed as the phase average stresses of the Composite Cylinder Assemblage. The matrix plasticity is treated by a transversely isotropic J_2 theory with the exception that the response is found in an average sense since the onset of plastic flow (von Mises' yield surface) and the flow itself (Prager's Rule) are based on the matrix phase average stresses. The hardening is temperature-dependent and kinematic. The mathematical model also accounts for the temperature dependency of the fiber and matrix material properties.

The purpose of this work was to create an inexpensive but powerful analytical method capable of predicting the trends in the thermomechanical response of laminates with ductile matrices. Note that the method is not suitable for the detailed analysis of structures; for instance, the model does not account for time-dependent effects or micromechanical damage. But within the context of its limitations the model is a valuable tool for investigating and interpreting basic material behavior. The model is therefore highly useful in the development of experimental materials and in the assessment of prototype structure.

BACKGROUND

Supersonic and transatmospheric flight will cause high thermal loading of vehicle surfaces and propulsion systems. Metal matrix composites (MMC), because of their thermal conductivity, stiffness, strength, and tailorability are candidate materials of construction for particularly hot areas of these structures. In the technical maturation effort of the National Aerospace Plane program (NASP) the hardware of several of the demonstrator projects has been constructed of MMC. It is projected that MMC may constitute 10% of the material of supersonic aircraft.

In contrast to the desirable properties of MMC is the fact that these materials can respond inelastically. The source of the inelasticity is often the yielding of the matrix under moderate thermal loadings. In an MMC the fiber and matrix typically have greatly different thermal expansivities (the axial coefficient of thermal expansion for advanced graphite fibers is actually negative). Because of this mismatch in properties, thermal loadings cause a buildup of constituent stresses as the material tries to hold itself together. The induced stresses are high, and although the fiber response is linear elastic the matrix can undergo substantial plastic flow. When the thermal loads are removed the mismatch in thermal expansivity can cause yielding in reverse as the structure cools. The residual plastic strain that exists after a thermal cycle can grow with successive thermal exposures leading to a ratcheting of the thermal hysteresis loops. The possibility of high stress levels, low cycle fatigue, and unacceptable flight deformations are therefore pertinent design concerns.

A number of investigations have been directed toward studying the plasticity of MMC. Powerful numerical models (primarily based on the Finite Element Method) have been used to study yield surfaces,[1] nonlinear stress-strain response,[2] and ultimate strength.[3] Comparing the analytical results with experimental data indicates that plasticity theories can be used to predict much of the observed phenomena. However, numerical models by their detailed nature are not conducive to parametric analyses and can be expensive to apply in nonlinear problems that require iterative solutions.

In order to create useful engineering analysis tools a number of analytical models have been proposed. These models introduce approximations, primarily concerning the stress fields within the constituents, that make the analysis tractable but retain the salient features of elastic-plastic behavior. An early work in this area[4] considered a model of rigid fibers and an elastic-plastic power-law hardening matrix. The application of the model was limited to the estimate of transverse stress-strain behavior.

Another more general approach[5,6] is known as the Vanishing Fiber Diameter model (VFD) since it assumes that the presence of the fibers does not disturb the shear and transverse stress fields. By introducing matrix plasticity this model was used to compute composite yield surfaces and composite plastic flow. The VFD performs well for plane stress loadings but is limited in its ability to analyze the effects of thermal loads. A similar approach[7] considered a two-dimensional VFD coupled with a White-Blesseling matrix plasticicity model in which the matrix response is treated by a number of subelements that behave elastic-perfectly-plastic. This model was used to examine cyclic thermal loadings but could not account for the evvect of a full three-dimensional stress state on the plastic response and was limited to materials with temperature-independent material properties. Note that after an analytical layer model is devised it is a straightforward procedure to construct an incremental laminate model from laminated plate theory.[8,9]

The work presented here is based on the Phase Average model,[10,11] which differs from the previous models in that it utilizes the Composite Cylinder Assemblage[12] to compute effective composite properties. This approach considers a full three-dimensional stress state and was used with success in a previous nonlinear laminate analysis[13] that examined the thermal hysteresis of aluminum MMC. This earlier effort is extended here to include temperature-dependent properties for both the fiber and the matrix and a transversely isotropic plasticity model with temperature-dependent hardening.

THEORETICAL DEVELOPMENT

The formulation starts with the development of a unidirectional layer model for both elastic and elastic-plastic response and then utilizes this model in the development of a general laminate stiffness relation.

UNIDIRECTIONAL MODEL

ELASTIC RESPONSE

The constitutive rate equations for transversely isotropic fibers and matrices are

$$\dot{\varepsilon}_{ij}^{FE} = S_{ijkl}^{FE}\,\dot{\sigma}_{kl}^{F} + \beta_{ij}^{FE}\,\dot{T} \tag{1}$$

$$\dot{\varepsilon}_{ij}^{ME} = S_{ijkl}^{ME}\,\dot{\sigma}_{kl}^{M} + \beta_{ij}^{ME}\,\dot{T} \tag{2}$$

where the S_{ijkl} are fourth-order compliance tensors, the β_{ij} are second-order equivalent thermal expansion tensors, the ϵ_{ij} are phase-average strains, the σ_{ij} are phase-average stresses, and T is the temperature. The overdot indicates the quantity is a rate term, the superscripts F and M refer to a fiber and matrix quantity, and the superscript E indicates that the quantity is elastic. The indices 1, 2, and 3 are principal material directions with 1 being directed along the axis of the fibers. The equivalent thermal expansion tensors are computed from

$$\beta_{ij}^{FE} = S_{ijkl,T}^{FE}\,\sigma_{kl}^{F} + \alpha_{ij}^{F} + \alpha_{ij,T}^{T}\,(T - T_o) \tag{3}$$

$$\beta_{ij}^{ME} = S_{ijkl,T}^{ME}\,\sigma_{kl}^{M} + \alpha_{ij}^{M} + \alpha_{ij,T}^{T}\,(T - T_o) \tag{4}$$

where the α_{ij} are the secant thermal expansivities, T_o is a reference temperature, and a comma denotes differentiation with respect to the listed variable.

The effective composite properties are computed through the Composite Cylinder Assemblage (CCA) as

$$S_{ijkl}^{*E} = f_1(V_F,\, S_{ijkl}^{FE},\, S_{ijkl}^{ME}) \tag{5}$$

$$\alpha_{ij}^{*E} = f_2(V_F,\, S_{ijkl}^{FE},\, S_{ijkl}^{ME},\, \alpha_{ij}^{F},\, \alpha_{ij}^{M}) \tag{6}$$

where the superscript * indicates a composite quantity, the functions f_1 and f_2 refer to the mathematical operations of the micromechanical model, and V_F is the fiber volume fraction. The constitutive law for the composite is therefore

$$\dot{\varepsilon}_{ij}^{*E} = S_{ijkl}^{*E}\,\sigma_{kl}^{*} + \beta_{ij}^{*E}\,\dot{T} \tag{7}$$

where

$$\beta_{ij}^{*E} = S_{ijkl,T}^{*E}\,\sigma_{kl}^{*} + \alpha_{ij}^{*} + \alpha_{ij,T}^{*}\,(T - T_o) \tag{8}$$

ELASTIC-PLASTIC RESPONSE

It is assumed here that the matrix yields uniformly when the matrix phase average stress state reaches a strain energy of distortion equal to the corresponding energy at yield for simple tension. Therefore, the onset of plastic flow is determined by a von Mises yield condition expressed in terms of the matrix phase average stresses. For a kinematic bilinear work hardening material the yield function ϕ is then

$$\phi = \psi - 3k^2 \tag{9}$$

where ψ is the load function and k is the strength parameter. The load function is computed from

$$\psi = (S_{ij}^{M} - h\,\varepsilon_{ij}^{MP})(S_{ij}^{M} - h\,\varepsilon_{ij}^{MP}) \tag{10}$$

where the S_{ij}^{M} are the deviatoric stresses computed from the phase average stresses, h is a hardening parameter, and the superscript P is used to designate a plastic quantity. The hardening parameter is computed from

$$h = 2/3\,\frac{E\,E_{\tan}}{E - E_{\tan}} \tag{11}$$

where E and $E_{\tan}$ are the matrix elastic and tangential moduli. The strength parameter is related to the matrix uniaxial yield stress σ_y through

$$k^2 = 2/9\,\sigma_y^2 \tag{12}$$

Note that the usual rules for loading and unloading apply except that they are expressed in terms of the phase average matrix stresses.

The constitutive law for matrix plasticity is Prager's Flow Rule expressed in terms of the matrix phase average stresses. The phase average matrix plastic strain rates are therefore

$$\dot{\varepsilon}_{ij}^{MP} = S_{ijkl}^{MP}\,\dot{\sigma}_{kl}^{M} + \beta_{ij}^{MP}\,\dot{T} \tag{13}$$

where S_{ijkl}^{MP} is the fourth-order plastic compliance tensor

$$S_{ijkl}^{MP} = \frac{1}{3\,h\,k^2}\,(S_{ij}^{M} - h\,\varepsilon_{ij}^{MP})\,(S_{kl}^{M} - h\,\varepsilon_{kl}^{MP}) \tag{14}$$

and β_{ij}^{MP} is the plastic thermal expansion vector

$$\beta_{ij}^{MP} = -h_{,T}\, S_{ijkl}^{MP}\, \varepsilon_{kl}^{MP} - \frac{k_{,T}}{h\,k}\,(S_{ij}^{M} - h\,\varepsilon_{ij}^{MP}) \tag{15}$$

The total phase average strain rates are found through the superposition of the elastic and plastic components

$$\dot{\varepsilon}_{ij}^{M} = \dot{\varepsilon}_{ij}^{ME} + \dot{\varepsilon}_{ij}^{MP} \tag{16}$$

Substituting equations (2) and (12) into (16) leads to

$$\dot{\varepsilon}_{ij}^{M} = S_{ijkl}^{MT}\,\dot{\sigma}_{kl}^{M} + \beta_{ij}^{MT}\,\dot{T} \tag{17}$$

where

$$S_{ijkl}^{MT} = S_{ijkl}^{ME} + S_{ijkl}^{MP} \tag{18}$$

$$\beta_{ij}^{MT} = \beta_{ij}^{ME} + \beta_{ij}^{MP} \tag{19}$$

and the superscript T refers to a total quantity.

TRANSVERSELY ISOTROPIC APPROXIMATION

In this work the CCA is used to compute the effective elastic-plastic composite properties from the fiber and matrix constitutive laws. However, the CCA model is limited to transversely isotropic constituents whereas the plastic response can be fully anisotropic. Also the equivalent thermal expansion tensors (equations ((3), (4), and (15) can also yield responses more general than transversely isotropic. To overcome this difficulty approximations are introduced to reduce the response to transversely isotropic. Let the approximation be indicated by the rules g_1 and g_2 such that

$$\bar{S}_{ijkl}^{MP} = g_1(S_{ijkl}^{MP}) \tag{20}$$

$$\bar{\beta}_{ij}^{MP} = g_2(\beta_{ij}^{MP}) \tag{21}$$

$$\bar{\beta}_{ij}^{ME} = g_2(\beta_{ij}^{ME}) \tag{22}$$

$$\bar{\beta}_{ij}^{FE} = g_2(\beta_{ij}^{FE}) \tag{23}$$

where the overbar indicates the transversely isotropic approximation. The rules chosen for g_1 are

$$\bar{S}_{1111}^{MP} = S_{1111}^{MP} \tag{24a}$$

$$\bar{S}^{MP}_{1122} = S^{MP}_{1122} \tag{24b}$$

$$\bar{S}^{MP}_{1133} = S^{MP}_{1122} \tag{24c}$$

$$\bar{S}^{MP}_{2222} = S^{MP}_{2222} \tag{24d}$$

$$\bar{S}^{MP}_{2233} = S^{MP}_{2233} \tag{24e}$$

$$\bar{S}^{MP}_{3333} = S^{MP}_{2222} \tag{24f}$$

$$\bar{S}^{MP}_{2323} = \frac{.5}{S^{MP}_{2222} - S^{MP}_{2233}} \tag{24g}$$

$$\bar{S}^{MP}_{1313} = S^{MP}_{1212} \tag{24h}$$

$$\bar{S}^{MP}_{1212} = S^{MP}_{1212} \tag{24i}$$

where the usual symmetries hold and where all of the unaddressed terms vanish. The rules for g_2 are

$$\bar{\beta}^{MP}_{11} = \beta^{MP}_{11} \tag{25a}$$

$$\bar{\beta}^{MP}_{22} = \beta^{MP}_{22} \tag{25b}$$

$$\bar{\beta}^{MP}_{33} = \beta^{MP}_{22} \tag{25c}$$

with all other β terms vanishing (similar results are obtained for β^{FE}_{ij} and β^{ME}_{ij}).

For axial loads, thermal loads, or in-plane shear loads the g_1 rules yield exact results. Since thermal loads are the dominant loadings for the intended application the approximations are not compromising. Furthermore, it has been shown that for general loadings[13] the more severe approximation of isotropic plasticity yields tolerable errors. However, as with all analytical models, individual applications must be assessed against the underlying assumptions.

ELASTIC RESPONSE, TRANSVERSELY ISOTROPIC APPROXIMATION

Introducing the g_2 rules the constitutive relations for the fibers and matrices become

$$\dot{\varepsilon}_{ij}^{FE} = S_{ijkl}^{FE}\,\dot{\sigma}_{kl}^{F} + \bar{\beta}_{ij}^{FE}\,\dot{T} \tag{26}$$

$$\dot{\varepsilon}_{ij}^{ME} = S_{ijkl}^{ME}\,\dot{\sigma}_{kl}^{M} + \bar{\beta}_{ij}^{ME}\,\dot{T} \tag{27}$$

The effective thermal composite properties are then computed as

$$\bar{\beta}_{ij}^{*E} = f_2(V_F,\, S_{ijkl}^{FE},\, S_{ijkl}^{ME},\, \bar{\beta}_{ij}^{FE},\, \bar{\beta}_{ij}^{ME}) \tag{28}$$

so that

$$\dot{\varepsilon}_{ij}^{*E} = S_{ijkl}^{*E}\,\sigma_{kl}^{*} + \bar{\beta}_{ij}^{*E}\,\dot{T} \tag{29}$$

PLASTIC RESPONSE, TRANSVERSELY ISOTROPIC APPROXIMATION

Applying the g_1 rules to equation (13) leads to

$$\dot{\varepsilon}_{ij}^{MP} = \bar{S}_{ijkl}^{MP}\,\dot{\sigma}_{kl}^{M} + \bar{\beta}_{ij}^{MP}\,\dot{T} \tag{30}$$

so that

$$\dot{\varepsilon}_{ij}^{M} = \bar{S}_{ijkl}^{MT}\dot{\sigma}_{kl}^{M} + \bar{\beta}_{ij}^{MT}\,\dot{T} \tag{31}$$

where

$$\bar{S}_{ijkl}^{MT} = S_{ijkl}^{ME} + \bar{S}_{ijkl}^{MP} \tag{32}$$

and

$$\bar{\beta}_{ij}^{MT} = \bar{\beta}_{ij}^{ME} + \bar{\beta}_{ij}^{MP} \tag{33}$$

The effective elastic-plastic composite properties can now be computed as

$$S_{ijkl}^{*T} = f_1(V_F,\, S_{ijkl}^{FE},\, \bar{S}_{ijkl}^{MT}) \tag{34}$$

$$\beta_{ij}^{*T} = f_2(V_F,\, S_{ijkl}^{FE},\, \bar{S}_{ijkl}^{MT},\, \bar{\beta}_{ij}^{F},\, \bar{\beta}_{ij}^{MT}) \tag{35}$$

from which the composite elastic-plastic constitutive relation becomes

$$\dot{\varepsilon}_{ij}^{*} = S_{ijkl}^{*T}\,\dot{\sigma}_{kl}^{*} + \beta_{ij}^{*T}\,\dot{T} \tag{36}$$

LAMINATE MODEL

The constitutive relations (29) and (36) can now be used to build an incremental laminate model. In order to do so, consider a laminate of thickness *2t* with the midthickness reference surface located in the z=0 x-y plane of the right-handed coordinate system x-y-z (z is perpendicular to the laminate layering). Invoking the Love-Kirchoff hypothesis leads to

$$\dot{u}_x(x,y,z) = \dot{u}_x^o(x,y) - z\,\dot{u}_{z,x}^o(x,y) \tag{37}$$

$$\dot{u}_y(x,y,z) = \dot{u}_y^o(x,y) - z\,\dot{u}_{z,y}^o(x,y) \tag{38}$$

$$\dot{u}_z(x,y,z) = \dot{u}_z^o(x,y) \tag{39}$$

where the functions u_x^o, u_y^o, u_z^o, are the displacements of the reference surface. The strain rates corresponding to these displacements are

$$\dot{\varepsilon}_{xx} = \dot{\varepsilon}_{xx}^o + z\,\dot{K}_{xx} \tag{40}$$

$$\dot{\varepsilon}_{yy} = \dot{\varepsilon}_{yy}^o + z\,\dot{K}_{yy} \tag{41}$$

$$\dot{\gamma}_{xy} = \dot{\gamma}_{xy}^o + z\,\dot{K}_{xy} \tag{42}$$

where the midsurface strain rates are

$$\dot{\varepsilon}_{xx}^o = \dot{u}_{x,x}^o \tag{43}$$

$$\dot{\varepsilon}_{yy}^o = \dot{u}_{y,y}^o \tag{44}$$

$$\dot{\gamma}_{xy}^o = \dot{u}_{x,y}^o + \dot{u}_{y,x}^o \tag{45}$$

and the rates of curvature are

$$\dot{K}_{xx} = -z\ \dot{u}^{o}_{z,xx} \tag{46}$$

$$\dot{K}_{yy} = -z\ \dot{u}^{o}_{z,yy} \tag{47}$$

$$\dot{K}_{xy} = -z\ \dot{u}^{o}_{z,xy} \tag{48}$$

Condensing equations (40), (41), and (42) with matrix notation leads to

$$[\dot{\varepsilon}_x] = [\dot{\varepsilon}^{o}] + z\ [\dot{K}] \tag{49}$$

Equations (28) and (35) can also be expressed in terms of engineering strains and matrix notation as

$$[\dot{\varepsilon}_1] = [S]\,[\dot{\sigma}_1] + [\beta]\,\dot{T} \tag{50}$$

where, depending upon the state of the layer, $[S]$ and $[\beta]$ are either elastic or elastic-plastic matrices. Inverting this equation leads to

$$[\dot{\sigma}_1] = [Q]\,[\dot{\varepsilon}_1] + [\Gamma]\,\dot{T} \tag{51}$$

where $[Q]$ is the layer stiffness matrix and

$$[\Gamma] = -[Q]\,[\beta] \tag{52}$$

The stress and strain rates expressed in the local layer coordinate system can be transformed to the global plate coordinate system through

$$[\dot{\sigma}_x] = [\Theta_\sigma]\,[\dot{\sigma}_1] \tag{53}$$

$$[\dot{\varepsilon}_x] = [\Theta_\varepsilon]\,[\dot{\varepsilon}_1] \tag{54}$$

where the transformation matrices are

$$[\Theta_\sigma] = \begin{bmatrix} \cos^2\theta & \sin^2\theta & -2\sin\theta\cos\theta \\ \sin^2\theta & \cos^2\theta & 2\sin\theta\cos\theta \\ \sin\theta\cos\theta & -\sin\theta\cos\theta & \cos^2\theta - \sin^2\theta \end{bmatrix} \tag{55}$$

and

$$[\Theta_\varepsilon] = \begin{bmatrix} \cos^2\theta & \sin^2\theta & -\sin\theta\cos\theta \\ \sin^2\theta & \cos^2\theta & \sin\theta\cos\theta \\ 2\sin\theta\cos\theta & -2\sin\theta\cos\theta & \cos^2\theta - \sin^2\theta \end{bmatrix} \tag{56}$$

with θ being the angular orientation between the local 1 and the global x coordinate directions. Substituting equations (53) and (54) into equation (51) leads to

$$[\dot{\sigma}_x] = [\bar{Q}]\,[\dot{\varepsilon}_x] + [\bar{\Gamma}]\,\dot{T} \tag{57}$$

where $[\bar{Q}]$ and $[\bar{\Gamma}]$ are the global stiffness and thermal stress matrices computed from

$$[\bar{Q}] = [\Theta_\sigma]\,[Q]\,[\Theta_\varepsilon]^{-1} \tag{58}$$

and

$$[\bar{\Gamma}] = [\Theta_\sigma]\,[\Gamma] \tag{59}$$

From the laminate edge stress rates the following stress resultant rates are defined

$$(\dot{N}_{xx}, \dot{N}_{yy}, \dot{N}_{xy}) = \int_{-t}^{t} (\dot{\sigma}_{xx}, \dot{\sigma}_{yy}, \dot{\sigma}_{xy})\, dz \tag{60}$$

$$(\dot{M}_{xx}, \dot{M}_{yy}, \dot{M}_{xy}) = \int_{-t}^{t} (\dot{\sigma}_{xx}, \dot{\sigma}_{yy}, \dot{\sigma}_{xy})\, z\, dz \tag{61}$$

Switching to matrix notation and introducing equation (57) leads to

$$[\dot{N}] = \int_{-t}^{t} [\bar{Q}]\,[\dot{\varepsilon}]\, dz + \int_{-t}^{t} [\bar{Q}]\,[\dot{K}]\, z\, dz + \int_{-t}^{t} [\bar{\Gamma}]\,\dot{T}\, dz \tag{62}$$

$$[\dot{M}] = \int_{-t}^{t} [\bar{Q}]\,[\dot{\varepsilon}]\, z\, dz + \int_{-t}^{t} [\bar{Q}]\,[\dot{K}]\, z^2 dz + \int_{-t}^{t} [\bar{\Gamma}]\,\dot{T}\, z\, dz \tag{63}$$

which can be combined and rewritten in the familiar laminated plate matrix notation as

$$\begin{bmatrix} \dot{N} \\ \dot{M} \end{bmatrix} = \begin{bmatrix} A & B \\ B & D \end{bmatrix} \begin{bmatrix} \dot{\varepsilon} \\ \dot{K} \end{bmatrix} + \begin{bmatrix} \dot{N}_T \\ \dot{M}_T \end{bmatrix} \tag{64}$$

which is the structural stiffness equation. When the loading rates are specified this equation can be inverted to yield the global displacement rates.

PHASE AVERAGE MODEL

After equation (64) is solved the laminate equations and the constitutive relations can be used to determine the composite stress rates for each layer. The constituent phase average stresses are then computed through the Phase Average model. In this model the phase average stress and strain rates are related through

$$\dot{\sigma}^*_{ij} = V_F\, \dot{\sigma}^F_{ij} + V_M\, \dot{\sigma}^M_{ij} \tag{65}$$

$$\dot{\varepsilon}^*_{ij} = V_F\, \dot{\varepsilon}^F_{ij} + V_M\, \dot{\varepsilon}^M_{ij} \tag{66}$$

where

$$V_M = 1 - V_F \tag{67}$$

Equations (65) and (66) are a consequence of using the CCA as the micromechanical model.

For layers that are responding elastically the phase average equations can be combined with the constitutive relations to yield

$$V_M\,(S^{FE}_{ijkl} - S^{ME}_{ijkl})\,\dot{\sigma}^M_{kl} = (S^{FE}_{ijkl} - S^{*E}_{ijkl})\,\dot{\sigma}^*_{kl} + (V_F\,\overline{\beta}^{FE}_{ij} + V_M\,\overline{\beta}^{ME}_{ij} - \beta^{*E}_{ij})\,\dot{T} \tag{68}$$

For layers that are responding plastically equation (68) becomes

$$V_M\,(S^{FE}_{ijkl} - \overline{S}^{MT}_{ijkl})\,\dot{\sigma}^M_{kl} = (S^{FE}_{ijkl} - S^{*T}_{ijkl})\,\dot{\sigma}^*_{kl} + (V_F\,\overline{\beta}^{FE}_{ij} + V_M\,\overline{\beta}^{MT}_{ij} - \beta^{*T}_{ij})\,\dot{T} \tag{69}$$

These equations yield the matrix phase average stress rates. The fiber phase average stress rates can then be determined from equation (65).

APPLICATIONS

DESCRIPTION

The engine walls of the NASP vehicle will be subjected to extremely high heat fluxes. To devise a structure capable of withstanding the projected thermal loadings it has been proposed that the walls be designed as heat exchangers using a high thermal conductivity material that possesses high stiffness and strength. Copper, which has a high innate conductivity, has its stiffness, strength, and conductivity enhanced with the addition of advanced P130x graphite fibers. This copper-based MMC will be analyzed here assuming a fiber volume fraction of 50%. The estimated material properties for the fiber and matrix are listed in Tables 1 and 2.

The engine walls will be prechilled prior to flight from an assumed ambient atmospheric temperature of 20 deg C to the fuel temperature of -170 deg C. During flight the temperature of the engine walls are anticipated to reach 650 deg C. After the flight the walls will return to an ambient condition. In this work the described thermal cycle is analytically applied to both unidirectional and cross-ply P130x/copper laminates.

NUMERICAL IMPLEMENTATION

The theoretical model was developed in terms of rates. However, the application of the model is necessarily incremental with piecewise linearity assumed for each step of the analysis. This is an approximation since the system characteristics are temperature and stress dependent and can vary continuously over the course of a load step. To correct for this and for the approximations of the transversely isotropic assumptions, the numerical model iterates to predict the onset of yield and to determine the extent of plastic flow. An evaluation of the effectiveness of these numerical procedures can be found in reference 13.

An additional control over the accuracy of the analysis is the size of the load increments. Table 3 shows the results of a numerical study in which successively smaller temperature increments where used in the analysis of a unidirectional P130x/copper plate subjected to one thermal cycle. A continuous plot of the response of the plate for half-degree temperature increments is shown in Figure 1. (An explanation of the predicted response can be found in the following subsection, "P130x/Copper".) For temperature-dependent hardening the field variables converge with decreasing temperature increments while, as a consequence of the micromechanical model, the composite and matrix axial strains align.

Table 3 and Figure 1 also show the results of a temperature-independent hardening model. Note that this assumption introduces a slight deviation from the more general model at the high end of the temperature cycle but achieves convergence of the field variables at a larger temperature increment.

P130x/COPPER

The first problem to be considered is a unidirectional plate subjected to two successive thermal load cycles. Figure 2 is a plot of the composite axial strain for this structure in which the response is seen to be extremely nonlinear and hysteretic but with no ratcheting. The composite initially responds during precooling by contracting elastically. However, the matrix material yields at -23.2 deg C after which the fiber properties dominate. Hence, with further cooling the composite begins to grow axially. On heating, the matrix response is again elastic so that the composite continues to grow until yield occurs at -61.5 deg C. From here on the composite contracts until the changing axial and transverse material properties interact to produce thermal growth. At the high end of the thermal cycle the growth peaks. With cooling, the composite contracts elastically and then plastically (yielding at 630 deg C). Further cooling leads to axial growth. The next and successive thermal cycles lead to an identical response. Figure 3 plots the composite transverse strain in which it is seen that the nonlinearity is not as severe since the fiber and matrix thermal expansivities are of the same sign. A slight hysteresis is also evident here. Figures 4 and 5 plot the matrix plastic strains which occur isovolumetrically. Figures 6 and 7

Table 1. Fiber Material Properties.

P130x Graphite Fiber		
Temperature deg C	α_a $\mu\varepsilon$ *per deg C*	α_t $\mu\varepsilon$ *per deg C*
-200	-1.62	10.0
-100	-1.62	10.0
0	-1.62	10.0
20	-1.62	10.0
100	-1.60	10.8
200	-1.05	10.8
300	-.625	11.6
400	-.275	12.4
500	.100	12.6
600	.450	12.6
700	.815	12.6

α_a axial secant thermal expansion (reference temperature = 20 deg C)

α_t transverse secant thermal expansion

E_a = 938 GPa, axial extensional modulus

E_t = 19.3 GPa, transverse extensional modulus

v_a = 0.210, axial Poisson's ratio

v_t = 0.892, transverse Poisson's ratio

G_a = 17.9 GPa, axial shear modulus

Table 2. Matrix Material Properties.

Copper, OFHC Grade					
Temperature	E	ν	α	σ_y	E_{tan}
deg C	GPa		$\mu\varepsilon$ *per deg C*	MPa	Gpa
-200	137	.360	14.4	107.	8.77
-100	126	.355	15.3	86.4	8.29
0	118	.345	16.3	72.5	8.05
20	117	.343	16.5	70.0	8.00
100	114	.333	17.0	60.5	7.58
200	110	.322	17.4	52.0	6.94
300	106	.312	17.7	42.6	6.12
400	102	.307	18.1	31.5	5.14
500	98	.299	18.5	21.4	4.56
600	93	.288	19.0	15.1	4.00
700	88	.275	19.5	11.7	3.44

E extensional modulus

ν_a Poisson's ratio

α secant thermal expansion (reference temperature = 20 deg C)

σ_y yield stress

E_{tan} tangent modulus

Table 3. Numerical Study of a P130x/Copper Unidirectional Plate.

Temperature Dependent Hardening (1) (2)										
Step Size	CPU Time	-170 deg C			650 deg C			Cool Down		
deg C	Sec	$\varepsilon_{11}^{\bullet}$	ε_{11}^{M}	ε_{11}^{MP}	$\varepsilon_{11}^{\bullet}$	ε_{11}^{M}	ε_{11}^{MP}	$\varepsilon_{11}^{\bullet}$	ε_{11}^{M}	ε_{11}^{MP}
5.0	51	1.358	1.321	18.83	6.022	5.314	-97.60	-.8899	-2.166	-7.309
2.0	119	1.359	1.344	18.82	6.089	5.806	-97.22	-.7613	-1.272	-6.610
1.0	217	1.359	1.352	18.82	6.111	5.970	-97.10	-.7185	-.9737	-6.378
0.5	425	1.359	1.355	18.82	6.123	6.052	-97.03	-.6970	-.8247	-6.261

Temperature Independent Hardening (1) (2)										
Step Size	CPU Time	-170 deg C			650 deg C			Cool Down		
deg C	Sec	$\varepsilon_{11}^{\bullet}$	ε_{11}^{M}	ε_{11}^{MP}	$\varepsilon_{11}^{\bullet}$	ε_{11}^{M}	ε_{11}^{MP}	$\varepsilon_{11}^{\bullet}$	ε_{11}^{M}	ε_{11}^{MP}
5.0	49	1.369	1.369	18.96	6.444	6.444	-92.07	-.8999	-.8999	-6.143
2.0	112	1.370	1.370	18.93	6.512	6.512	-92.09	-.7653	-.7653	-6.144
1.0	213	1.370	1.370	18.92	6.535	6.535	-92.10	-.7205	-.7205	-6.144
0.5	418	1.371	1.371	18.92	6.547	6.547	-92.10	-.6980	-.7018	-6.148

(1) The exponent of the strains is -4.

(2) The computations were performed on a Sun Microsystem 3/280.

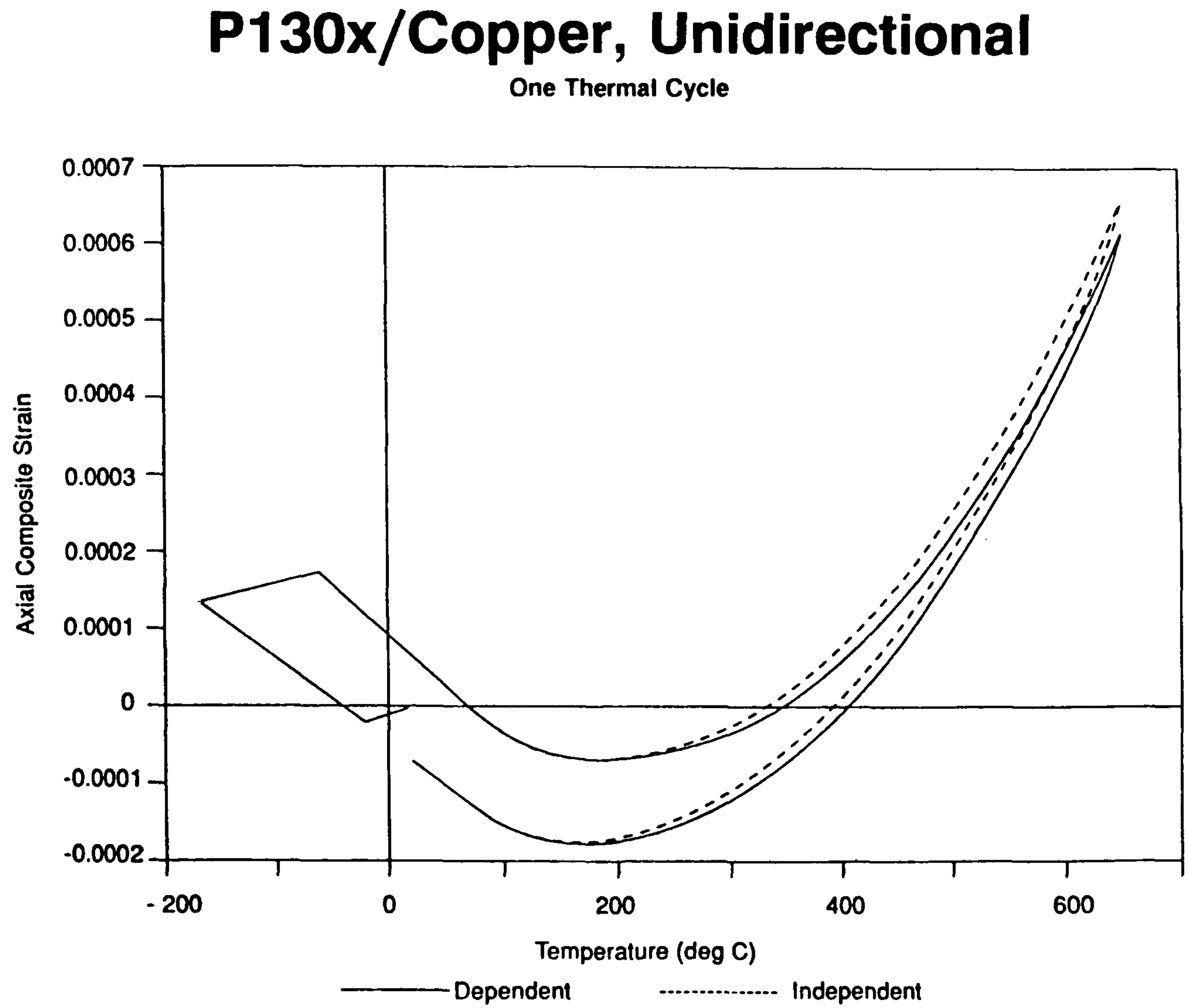

Figure 1. Composite Axial Strain vs. Temperature for Both Temperature-Dependent and Temperature-Independent Hardening.

show the matrix stresses caused by the mismatch in constituent straining. Note that in this problem the thickness matrix stress equals the transverse stress, while the shear stresses are zero.

Figure 8 plots the load function over the thermal cycle. This figure is useful in interpreting the different regions of thermoplastic response. During the initial cooling the matrix is elastically restrained by the fibers so that the load function quickly reaches the yield line along which it travels plastically. (The yield line is a plot of the strength term of equation (9).) Heating from the low temperature causes the load function to unload and reload elastically and then travel along the yield line plastically. In stress space this is equivalent to unloading from the yield surface, transversing the elastic region, and then striking the yield surface at another point. The same behavior occurs when the plate is cooled from the high temperature point. Subsequent cycles lead to identical results. Note that the effect of the temperature dependency is reflected in the length of the elastic path at the two temperature extremes.

Because of the method of manufacture MMC typically contains residual processing stresses. Although intuition would lead one to suspect that these stresses are tensile, there is evidence showing that surface friction and high processing pressures lead to residual stresses that are actually compressive. The second problem to be considered analyzes the effect of residual processing stresses on the thermal response by assuming a residual stress state of

$$(\sigma_{11}^M, \sigma_{22}^M, \sigma_{33}^M, \sigma_{12}^M, \sigma_{13}^M, \sigma_{23}^M) = (-80, -40, -40, 0, 0, 0)\, MPa$$

in a unidirectional plate. Figure 9 is a plot of the load function of this plate when it is subjected to two thermal cycles. The path starts at the residual stress state, unloads, reloads and then reaches the yield line at -60.8 deg C. The subsequent load path and the location of the yield points are virtually identical to the case with no residual processing stresses (Figure 8). Because of this the shape of the curves of the field variable in the residually stressed plate (Figures 10 through 15) are very similar to the plots of the initially unstressed plate. The difference in response is seen to be a vertical shift of the curves and hence the peak magnitudes. If a residual tensile stress state had been examined, then similar shifting would occur except in an opposite direction.

The next problem to be considered is a 0/90/90/0 cross-ply laminate (no residual stresses). Figure 16 shows that for such a structure the composite axial strains will ratchet under cyclic thermal loads. Because the construction is cross-plied and symmetrical, the transverse strains are identical to the axial strains. The matrix plastic strains (Figures 17 through 19) show a pronounced ratcheting. Since the construction constrains the plys from deforming individually, the thermal cycle will result in non-zero composite stresses. Figures 20 and 21 plot these composite stresses for the upper 0-deg ply. The matrix stresses are therefore a superposition of the effects of global composite stressing and of local differential thermal growth. Figures 22 through 24 show that these stresses ratchet substantially during the thermal cycle. Without the processes of stress relaxation, unacceptably high stress levels would soon be reached.

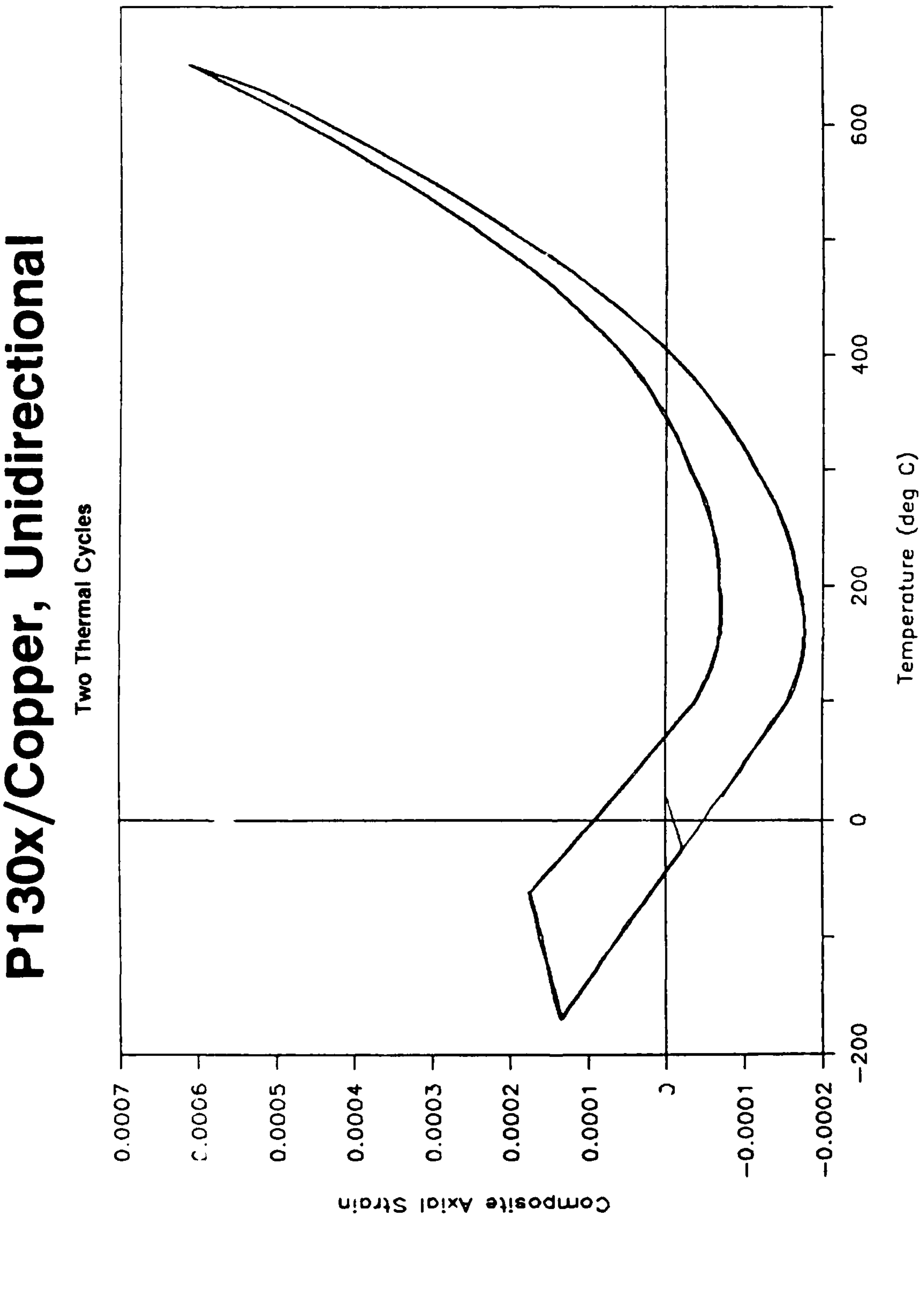

Figure 2. Composite Axial Strain vs. Temperature.

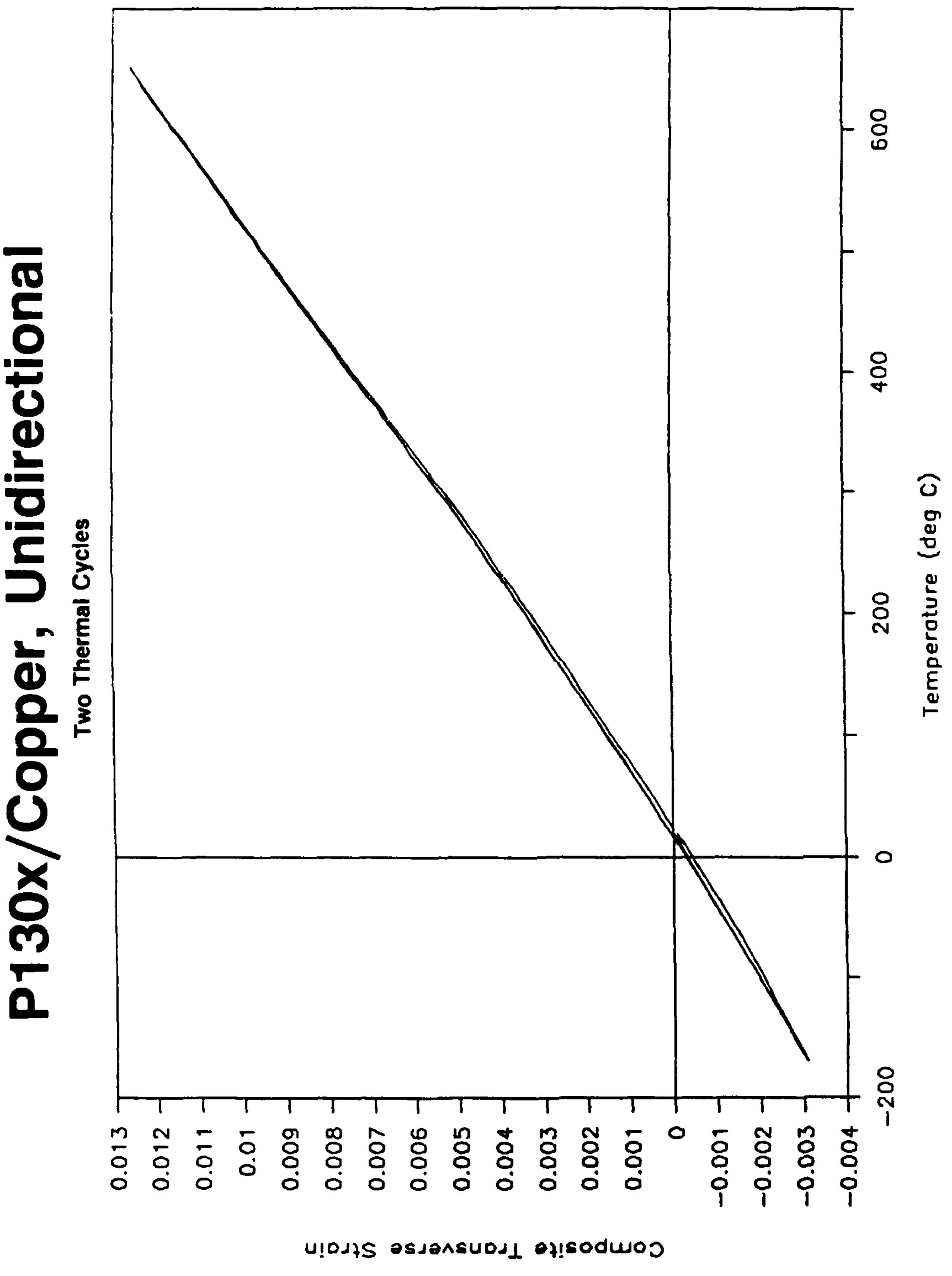

Figure 3. Composite Transverse Strain vs. Temperature.

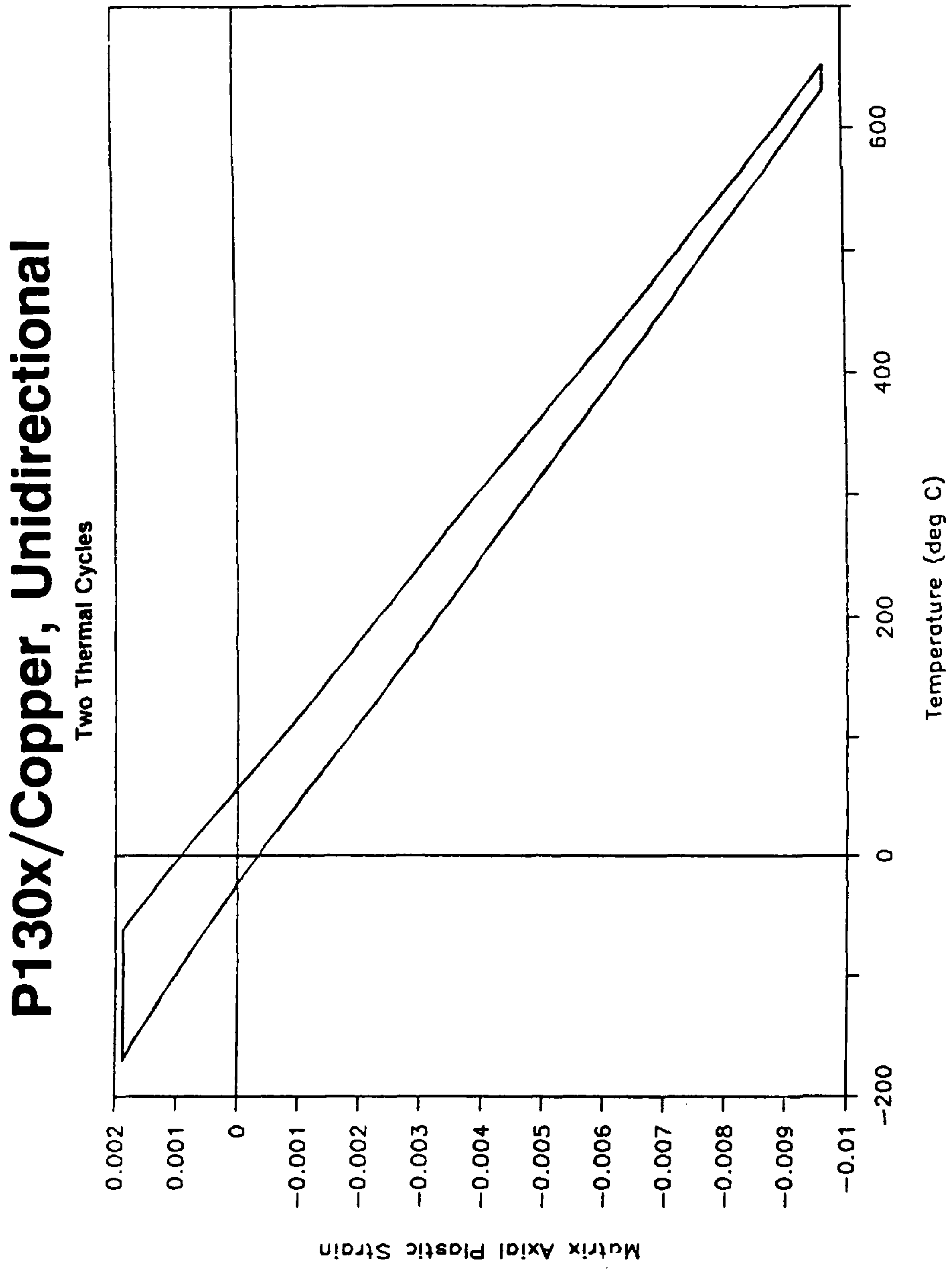

Figure 4. Matrix Axial Plastic Strain vs. Temperature.

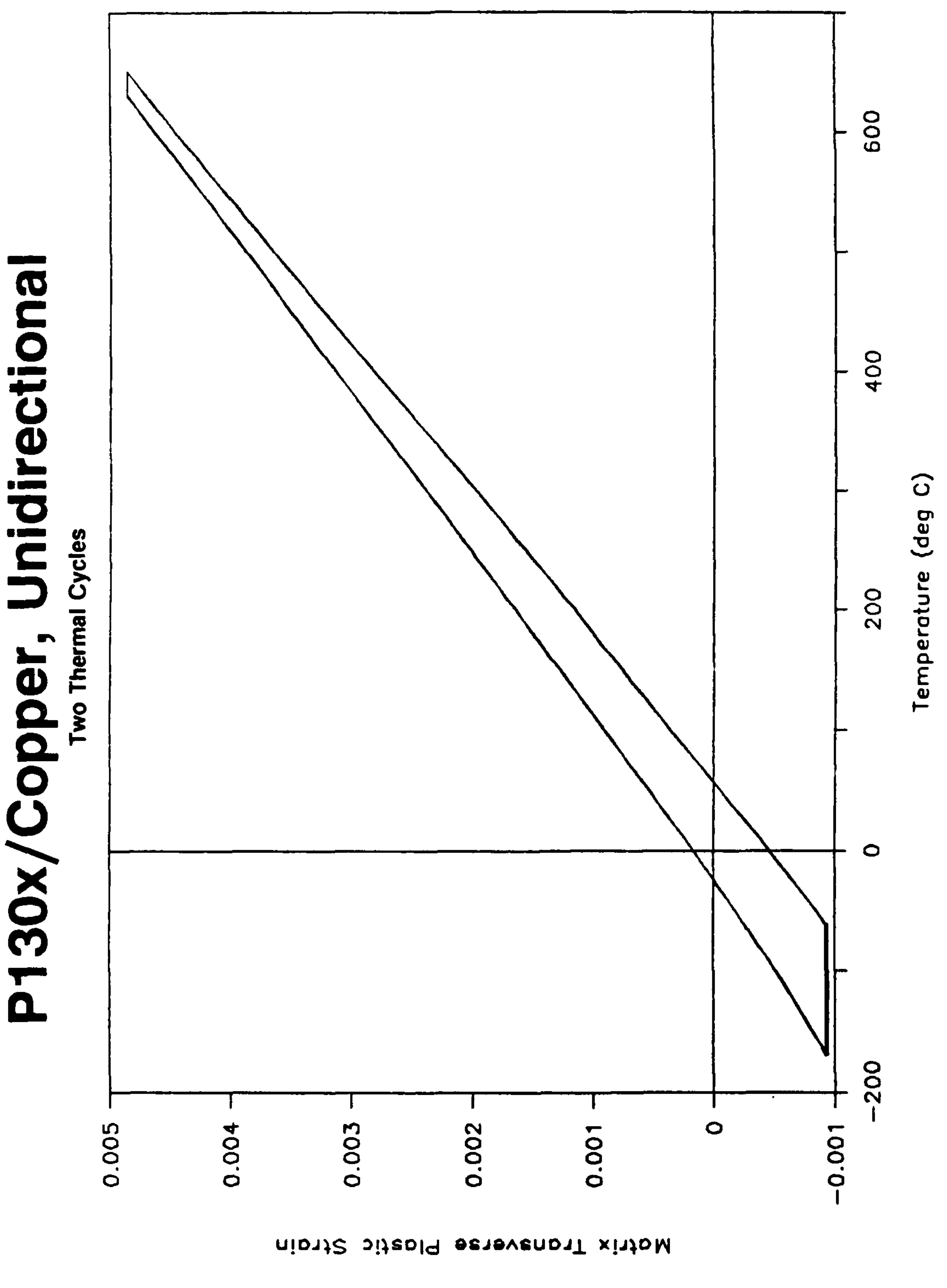

Figure 5. Matrix Transverse Plastic Strain vs. Temperature.

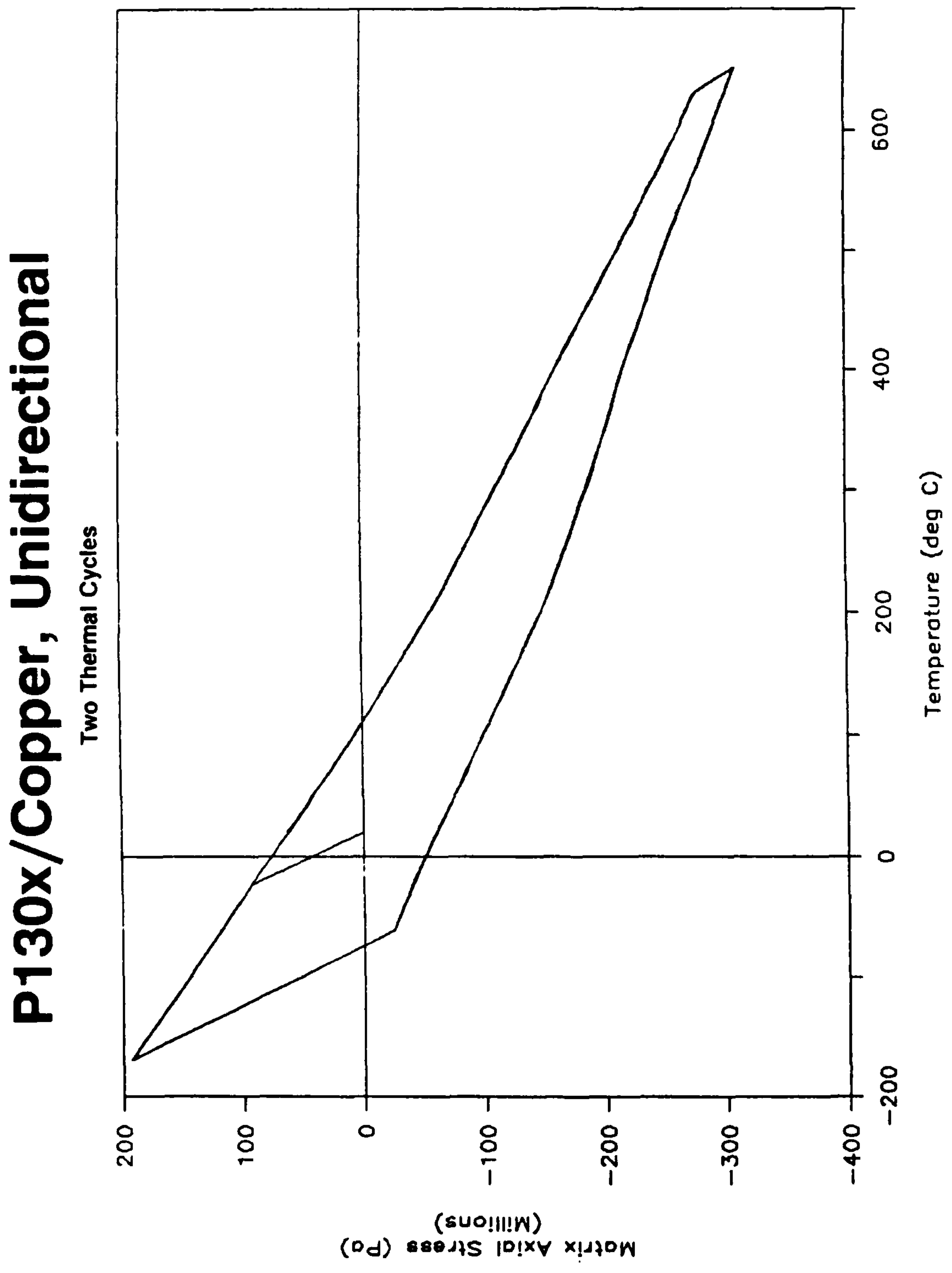

Figure 6. Matrix Axial Stress vs. Temperature.

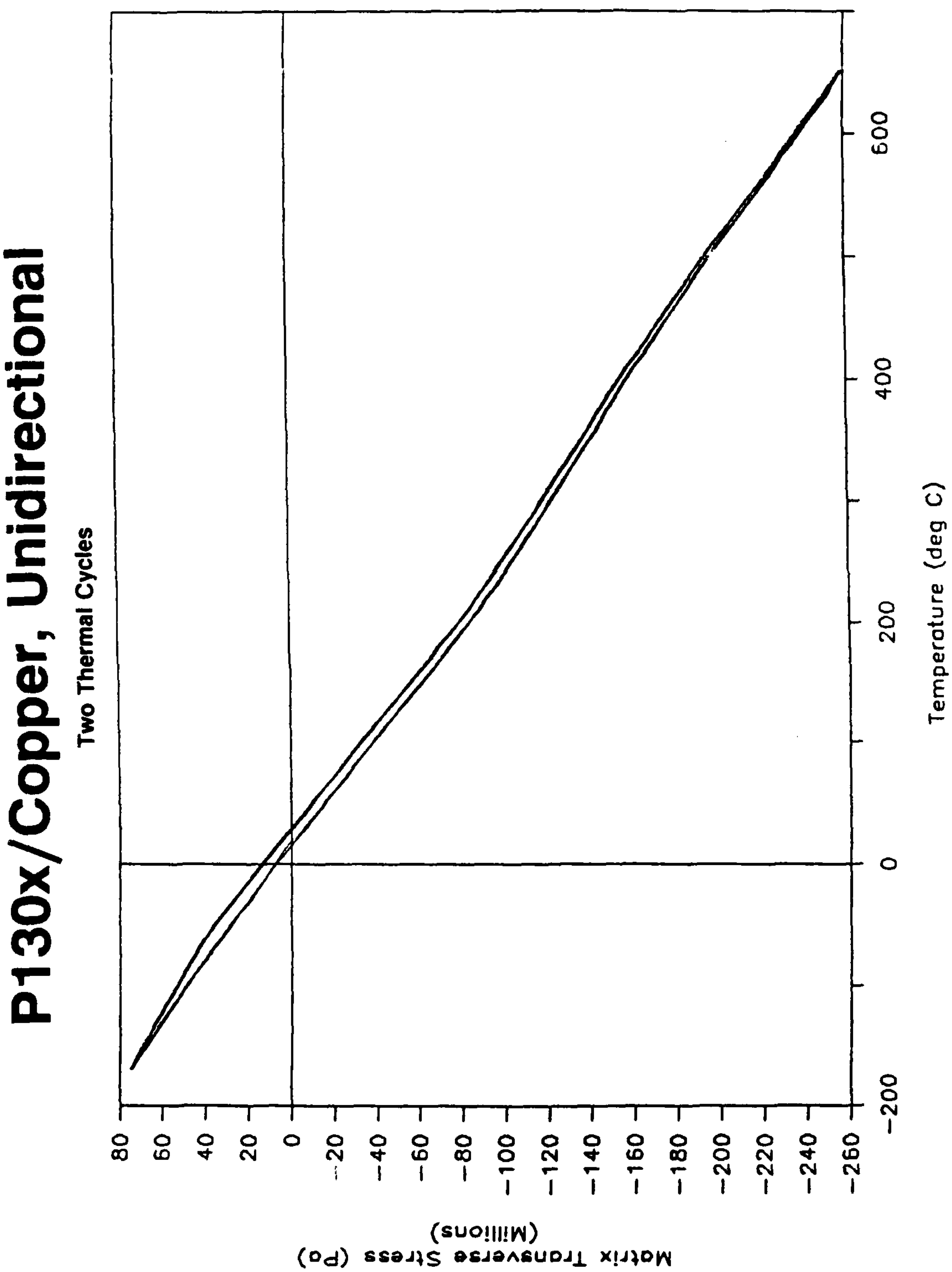

Figure 7. Matrix Transverse Stress vs. Temperature.

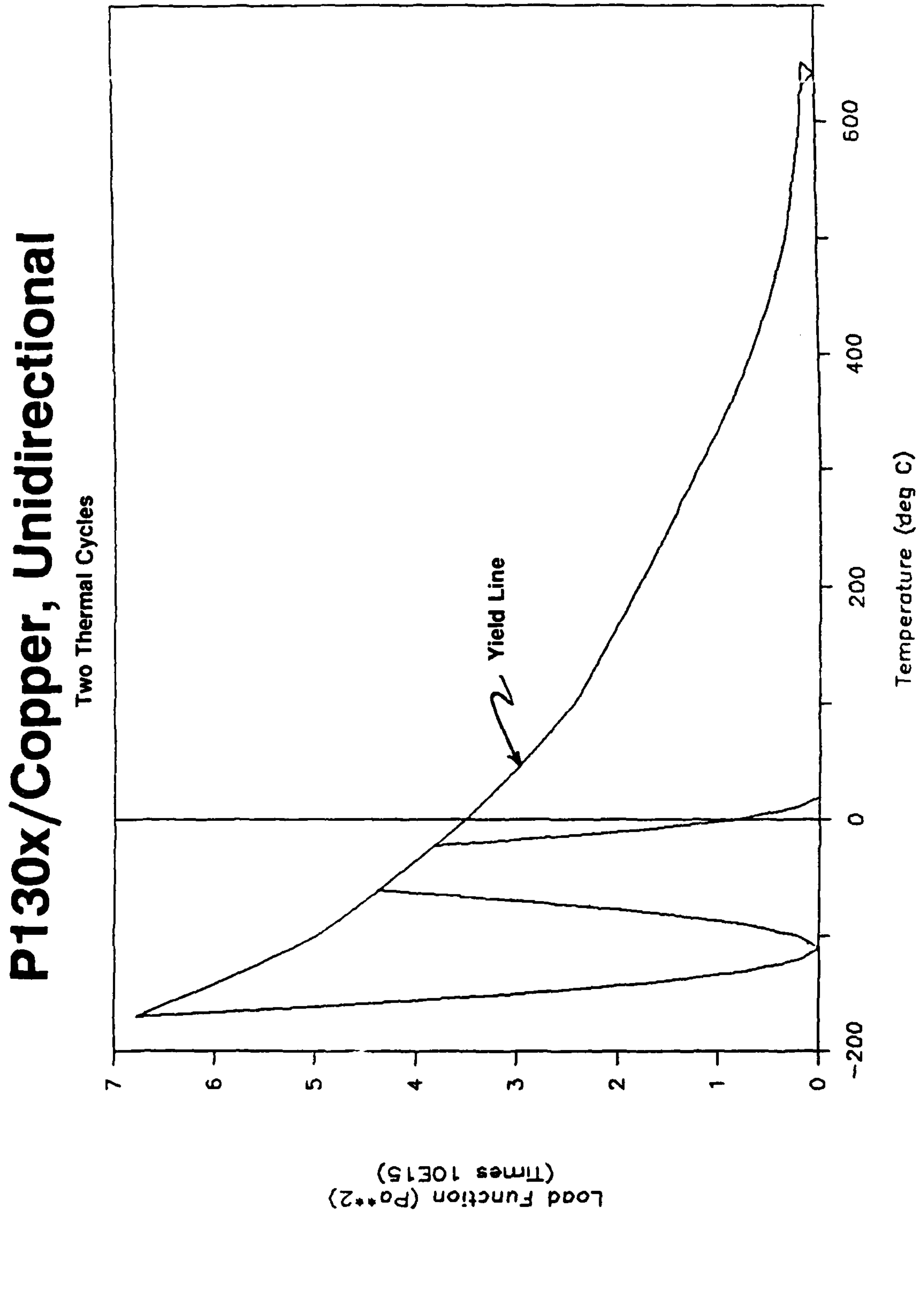

Figure 8. Load Function vs. Temperature.

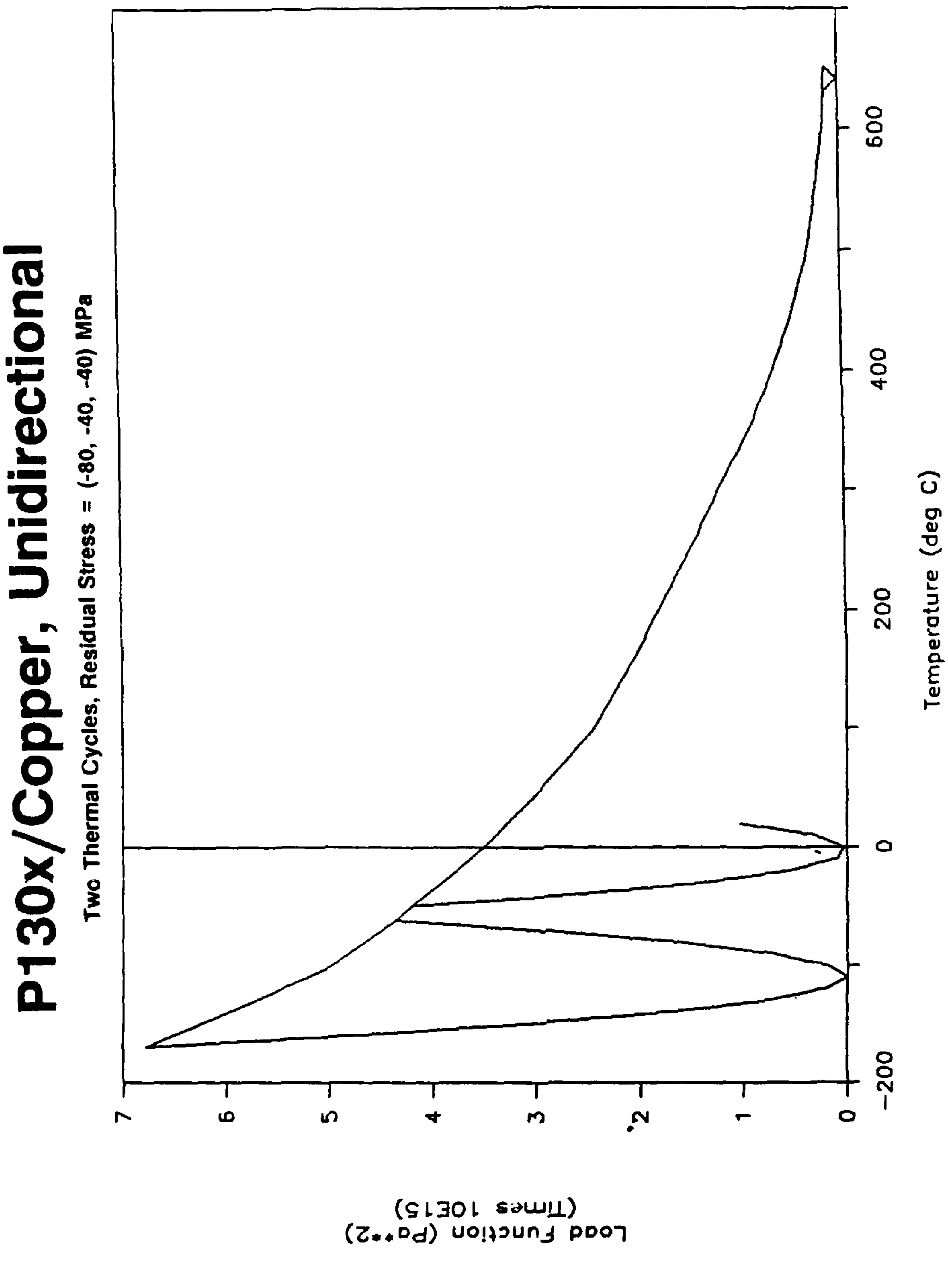

Figure 9. Load Function vs. Temperature.

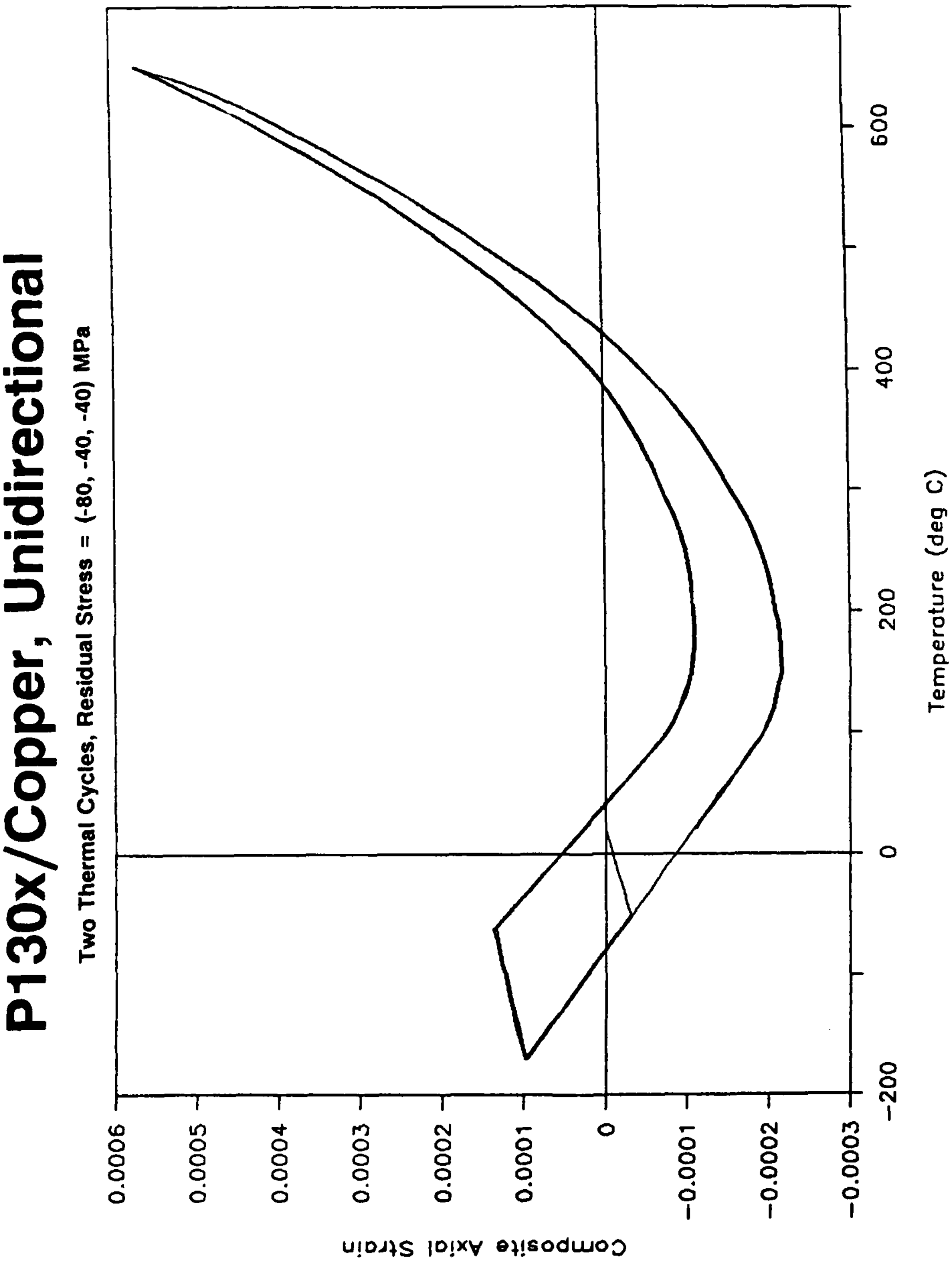

Figure 10. Composite Axial Strain vs. Temperature.

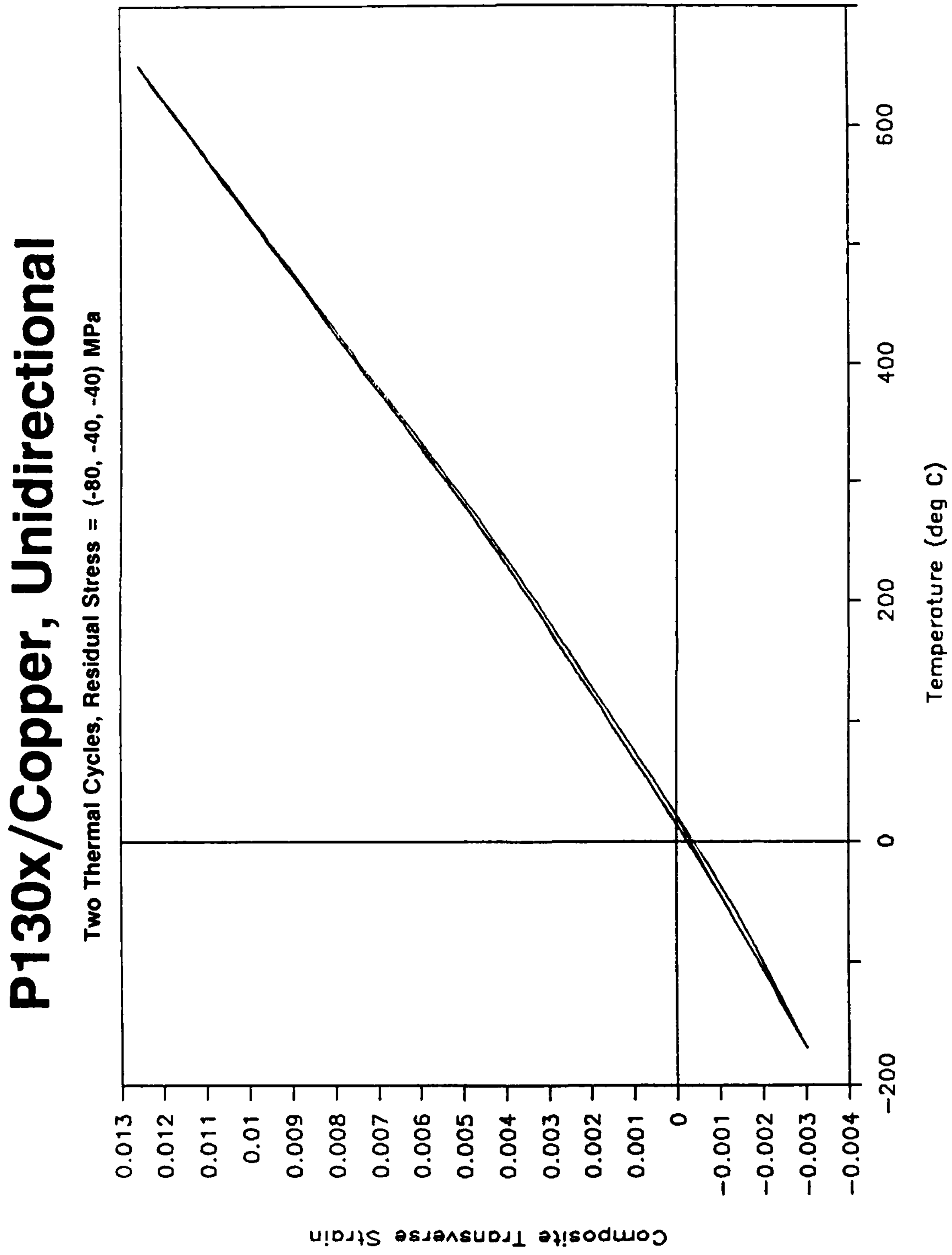

Figure 11. Composite Transverse Strain vs. Temperature.

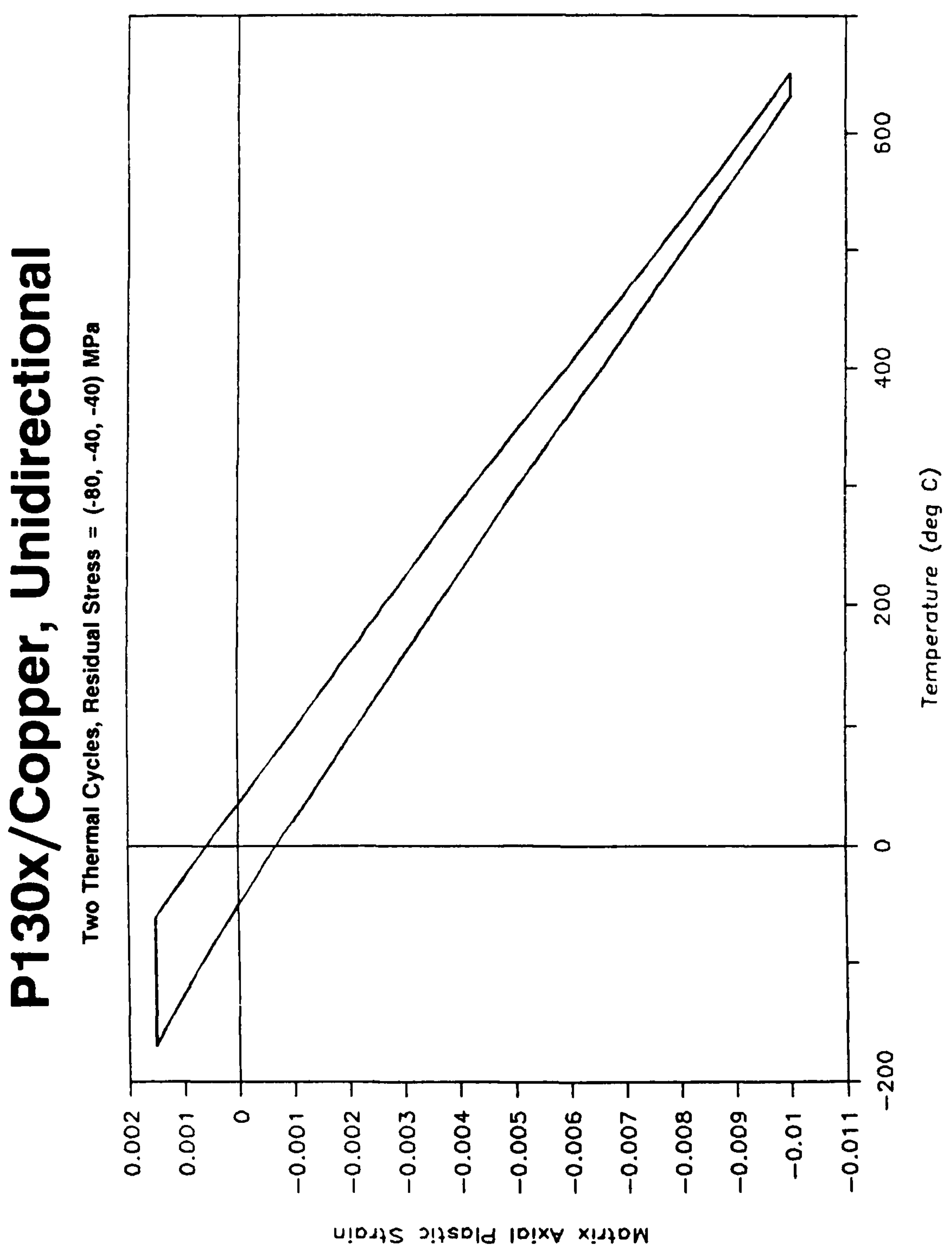

Figure 12. Matrix Axial Plastic Strain vs. Temperature.

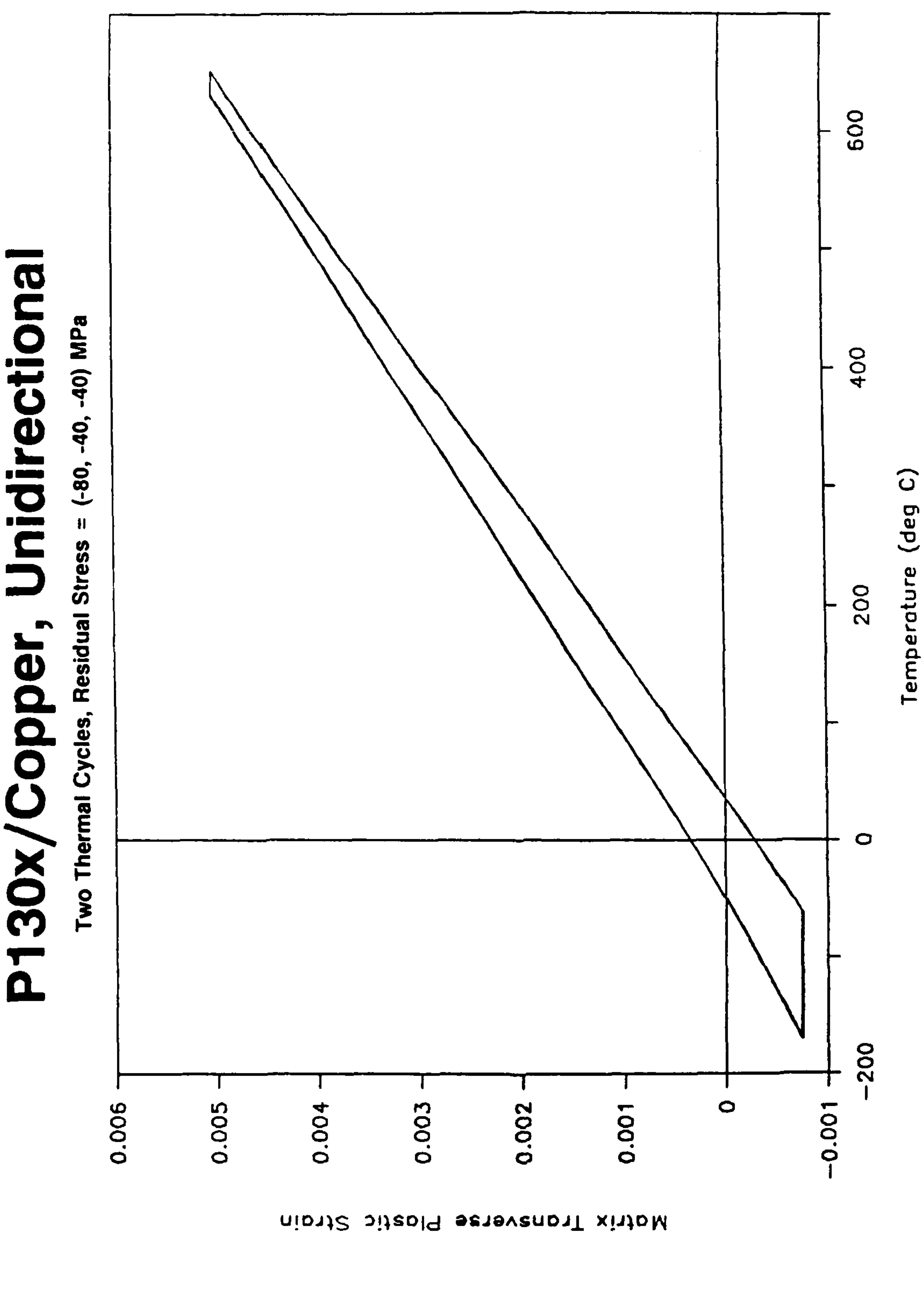

Figure 13. Matrix Transverse Plastic Strain vs. Temperature.

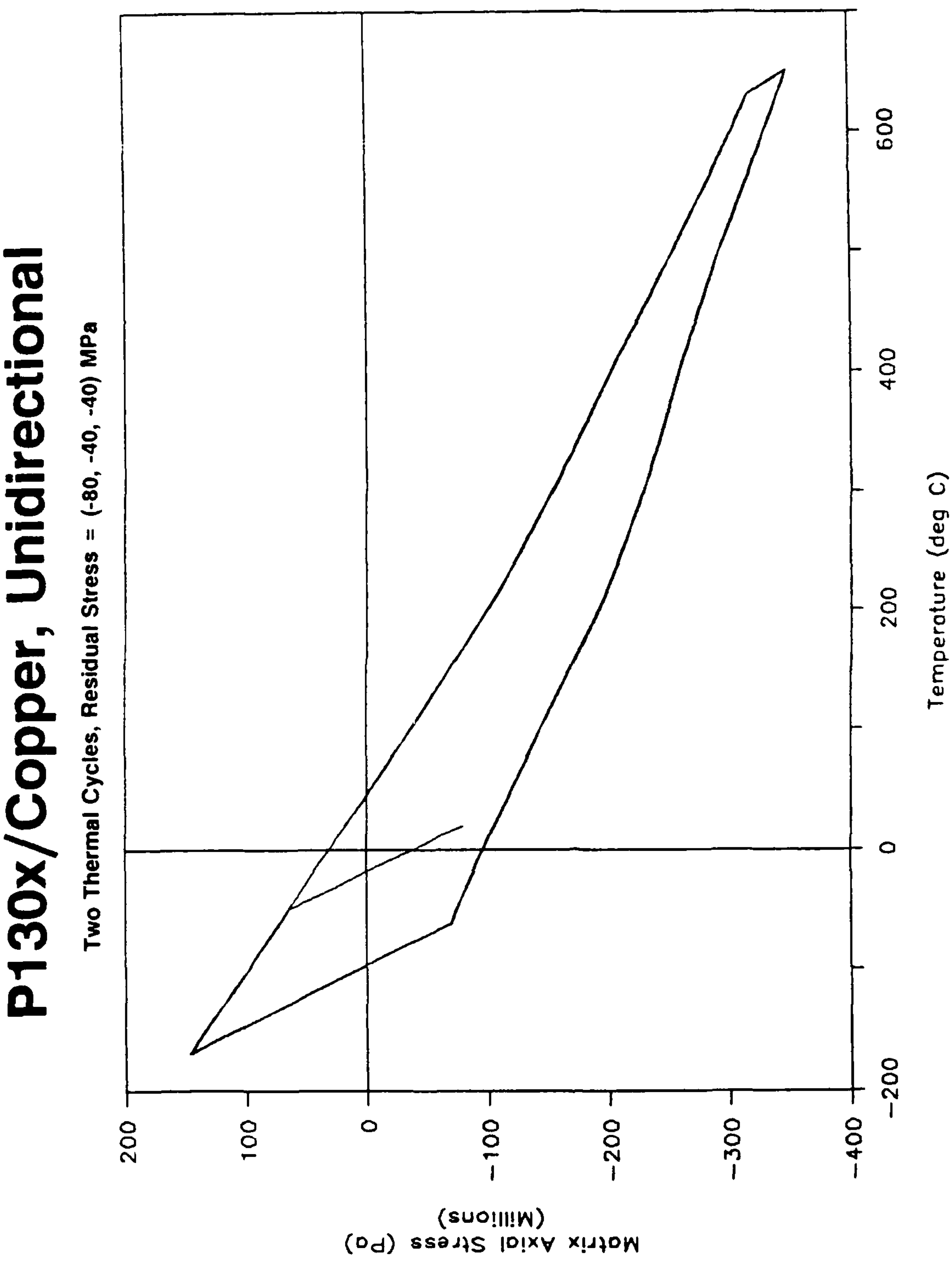

Figure 14. Matrix Axial Stress vs. Temperature.

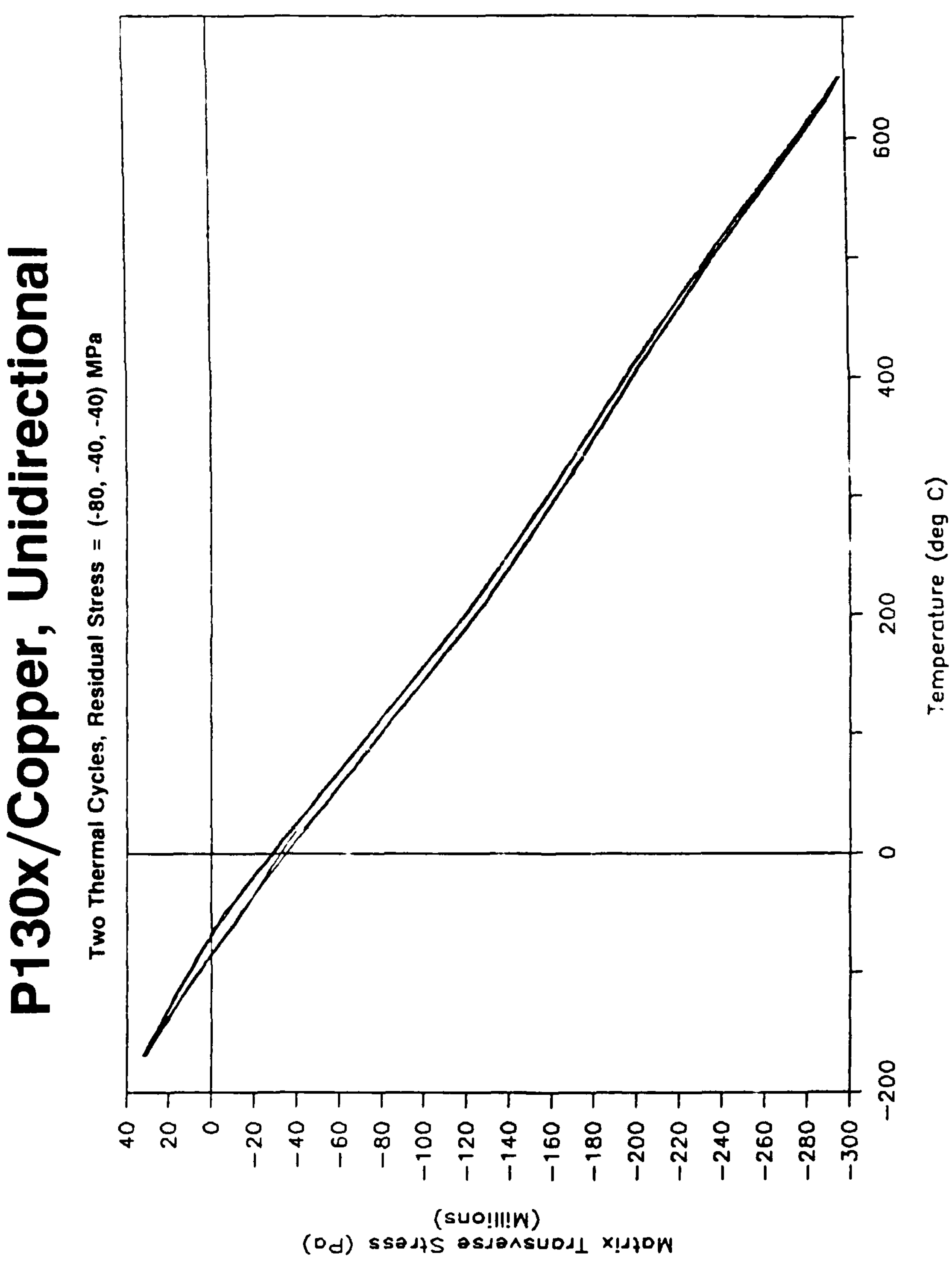

Figure 15. Matrix Transverse Stress vs. Temperature.

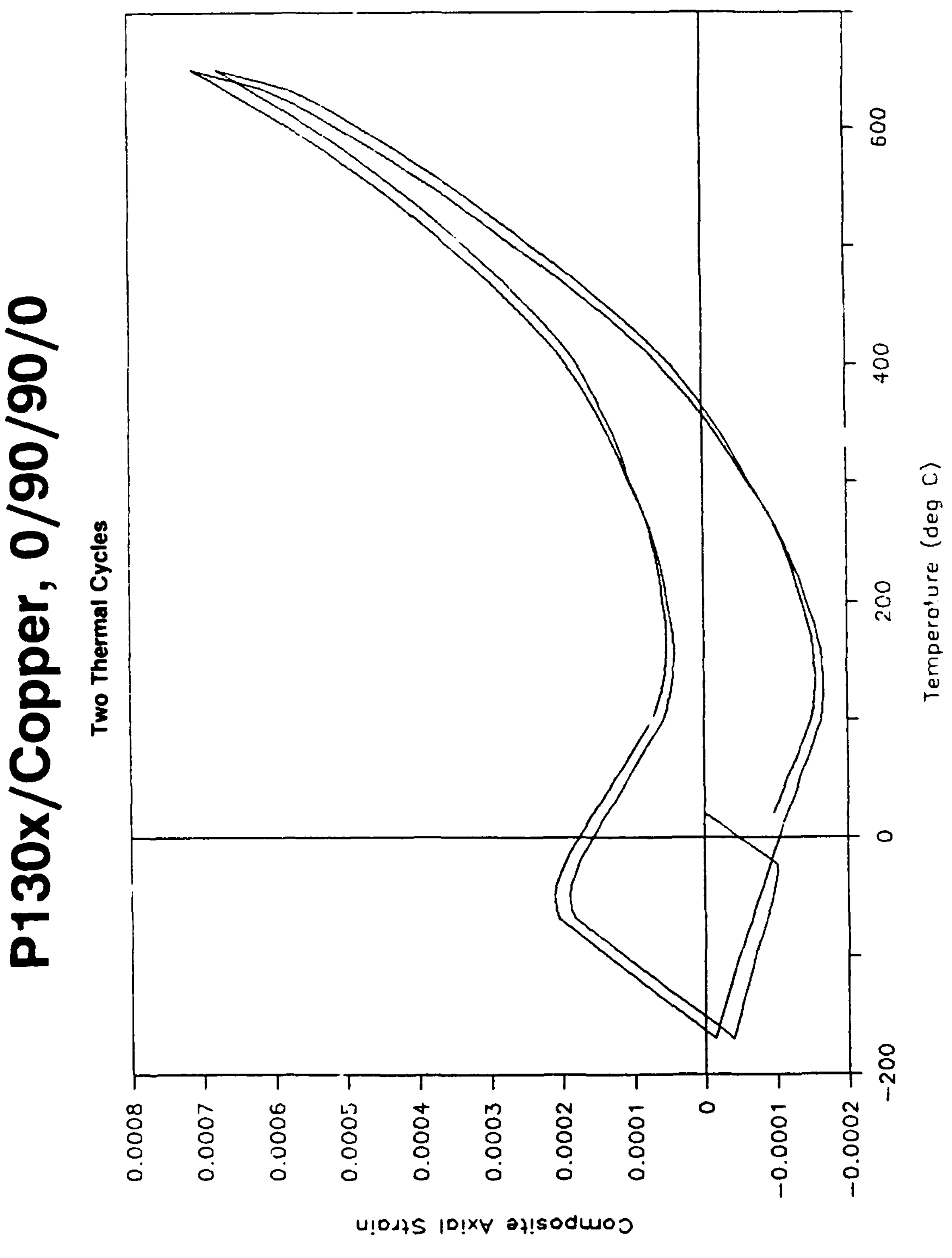

Figure 16. Composite Axial Strain vs. Temperature.

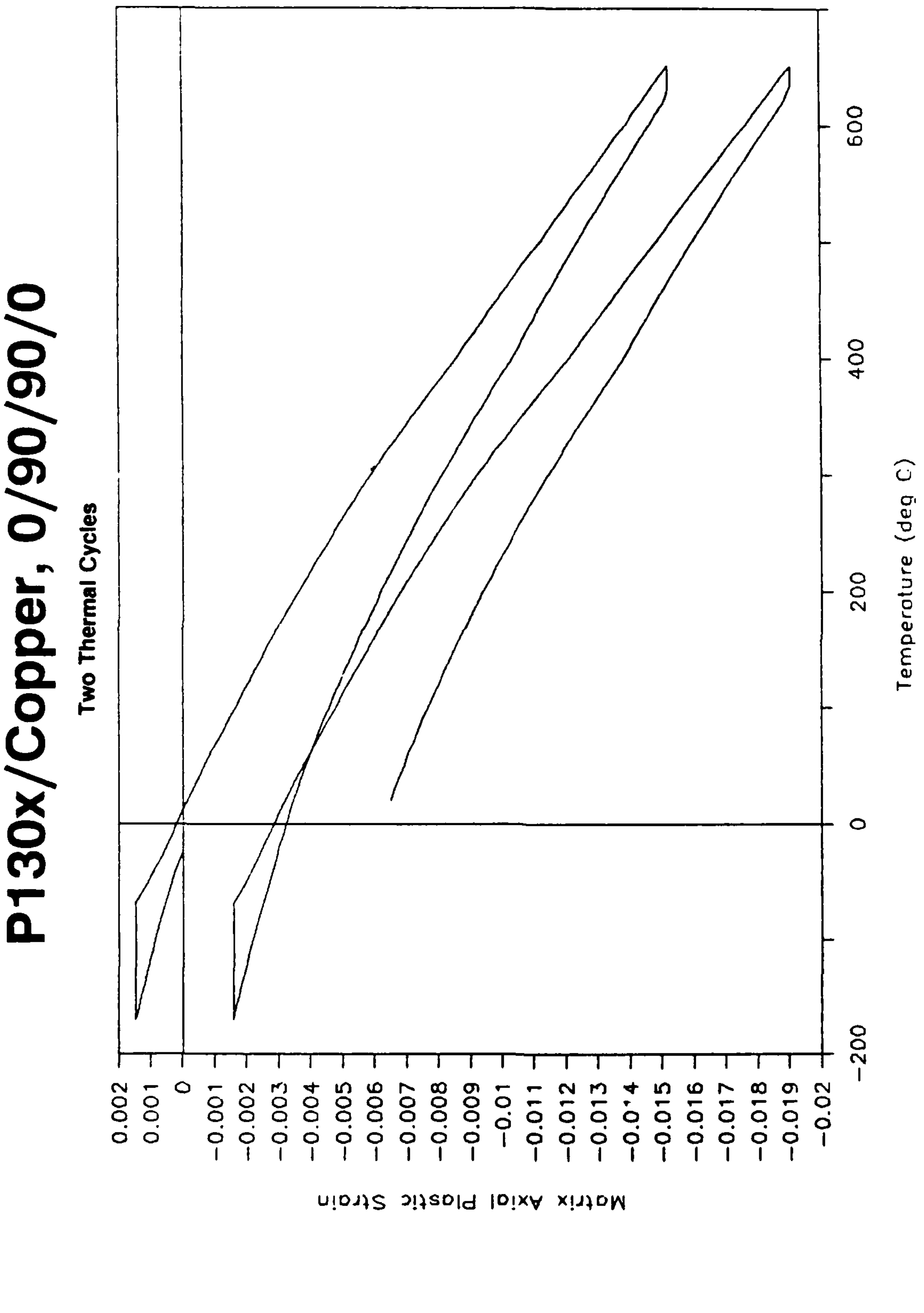

Figure 17. Matrix Axial Plastic Strain vs. Temperature.

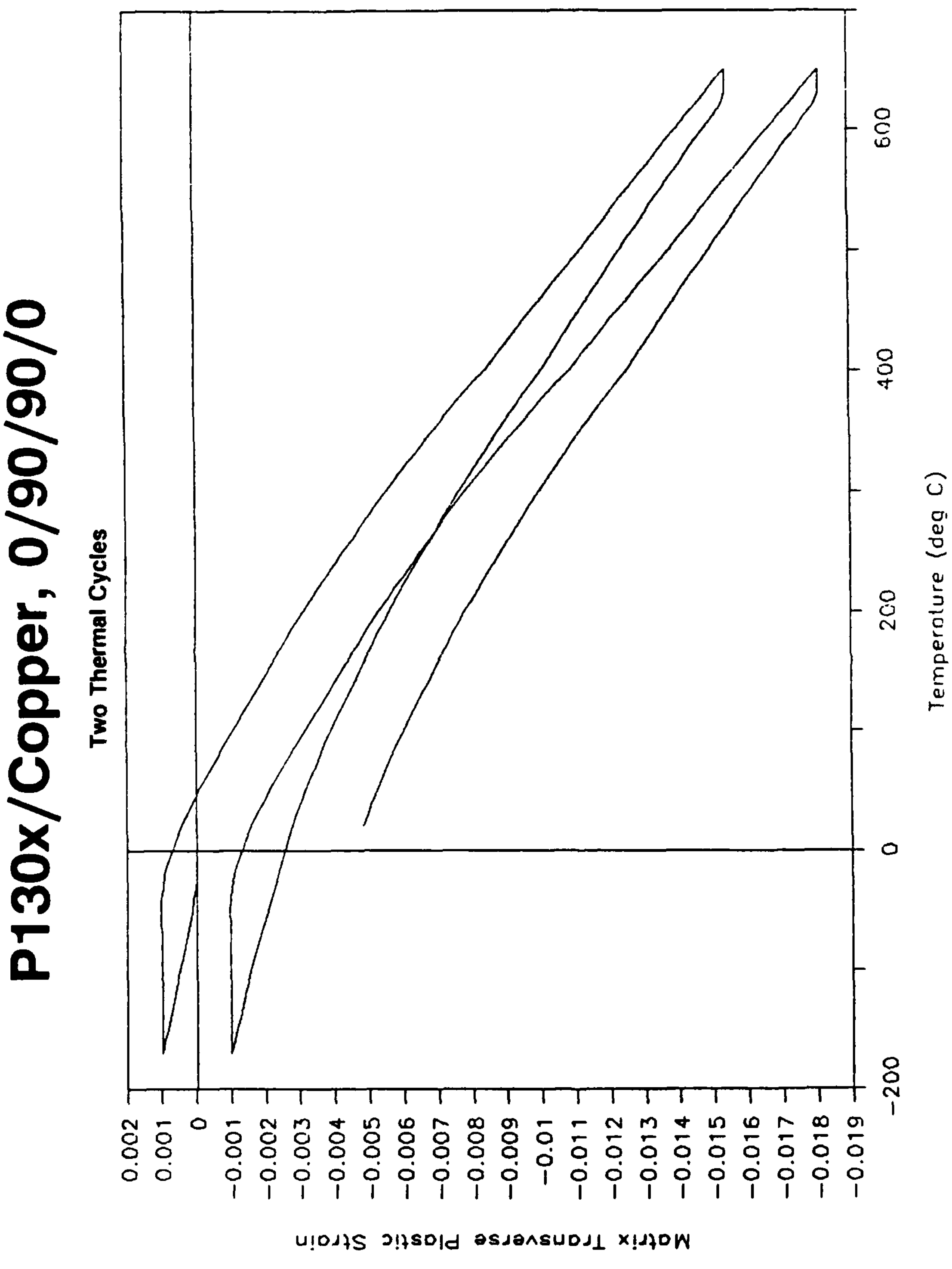

Figure 18. Matrix Transverse Plastic Strain vs. Temperature.

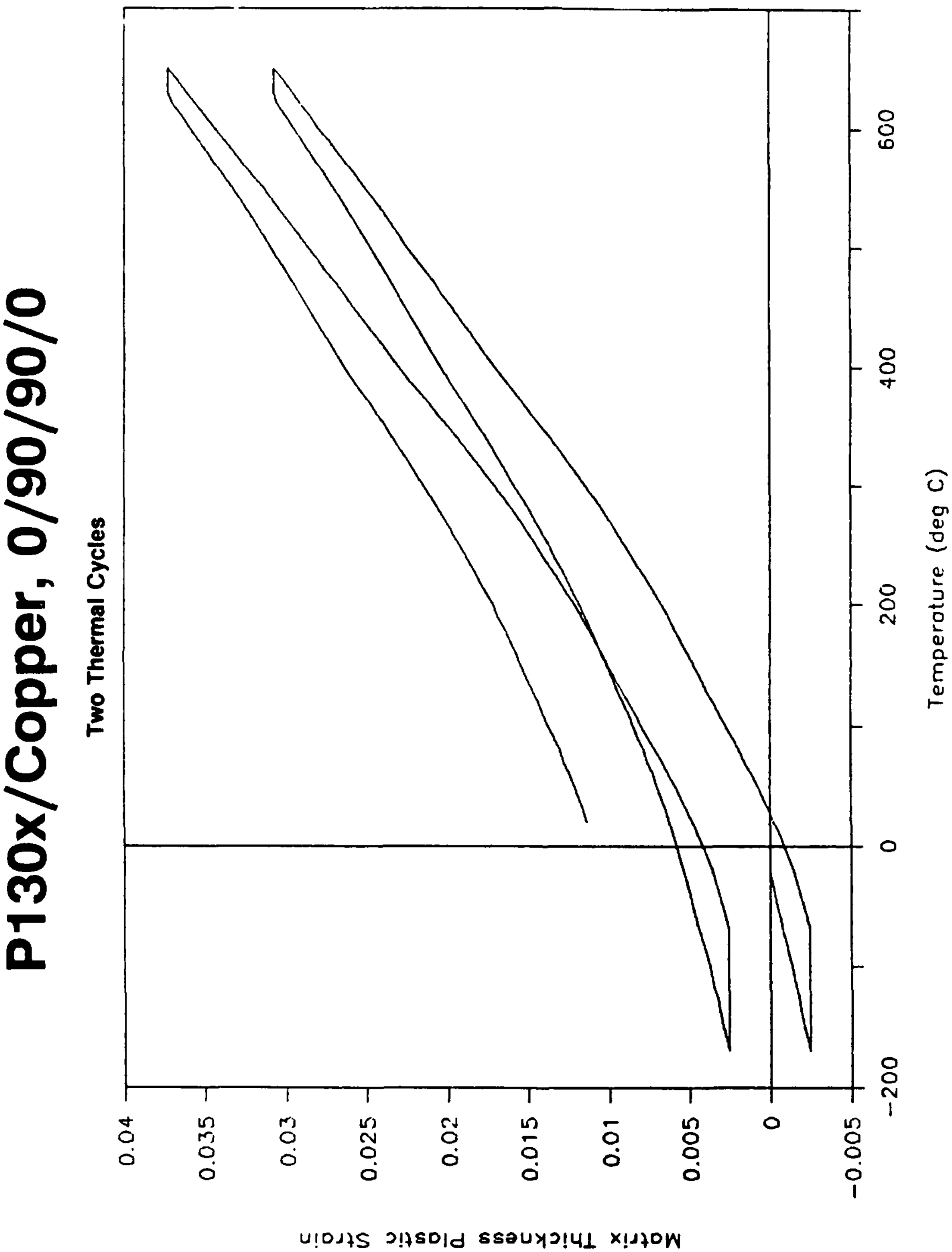

Figure 19. Matrix Thickness Plastic Strain vs. Temperature.

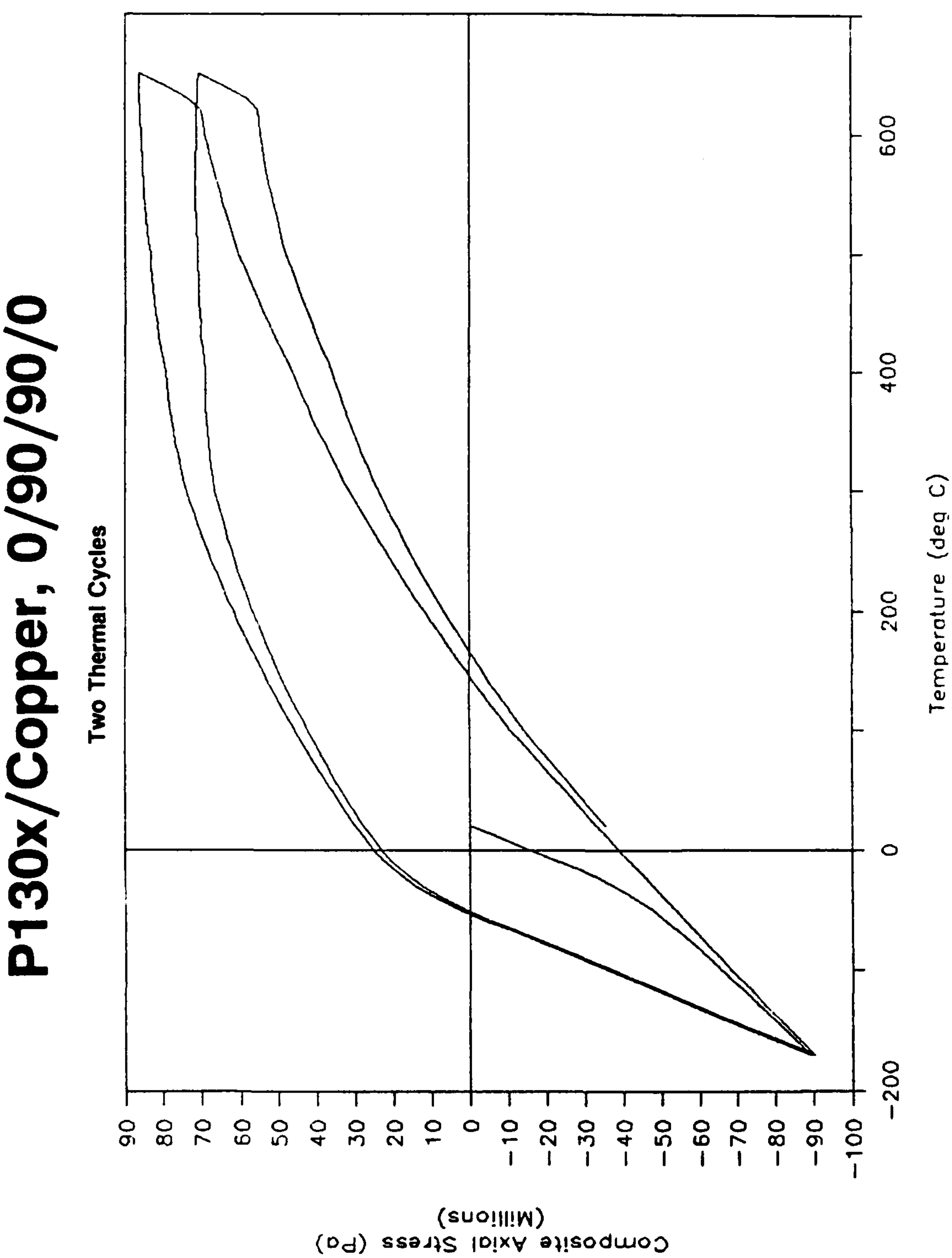

Figure 20. Composite Axial Stress vs. Temperature.

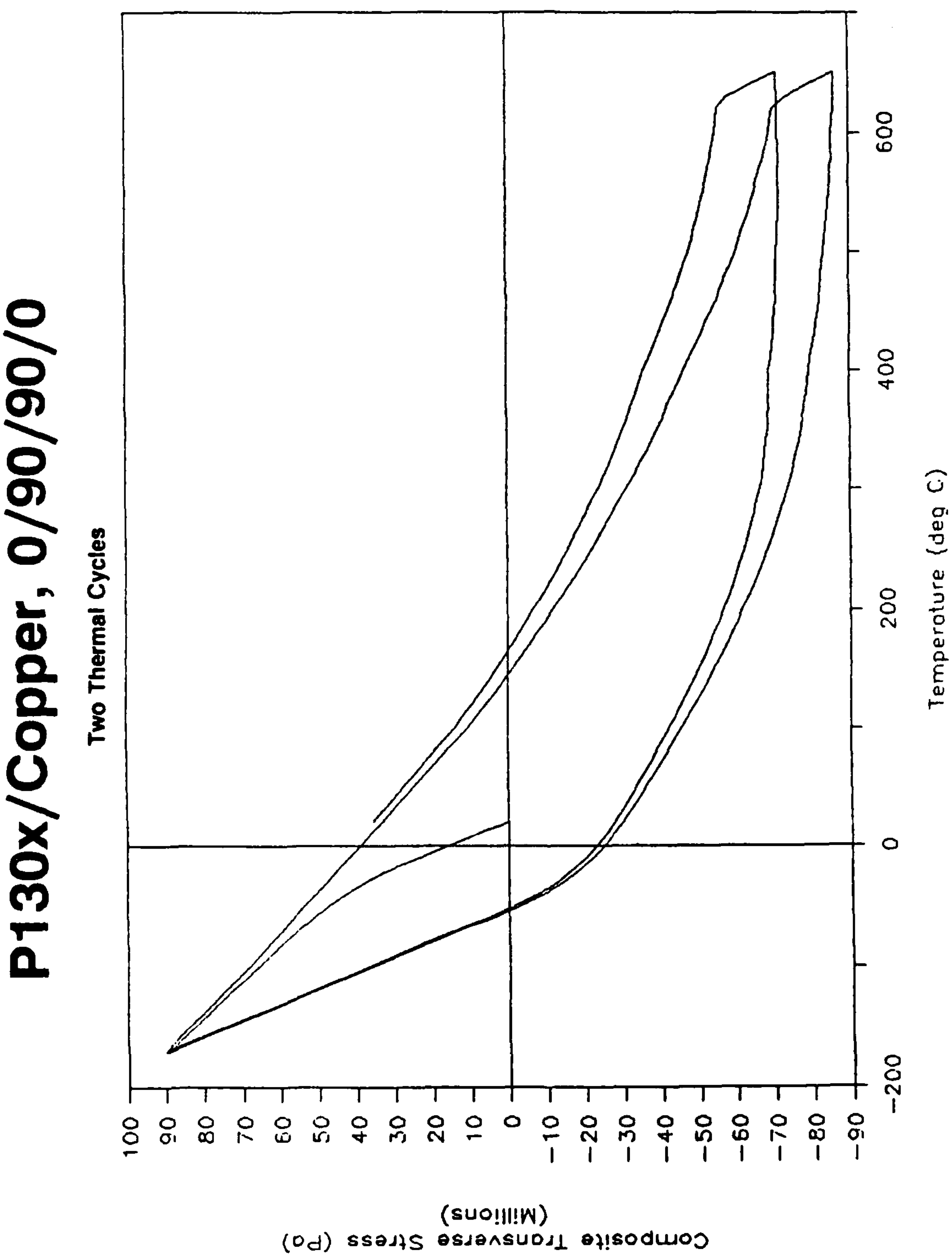

Figure 21. Composite Transverse Stress vs. Temperature.

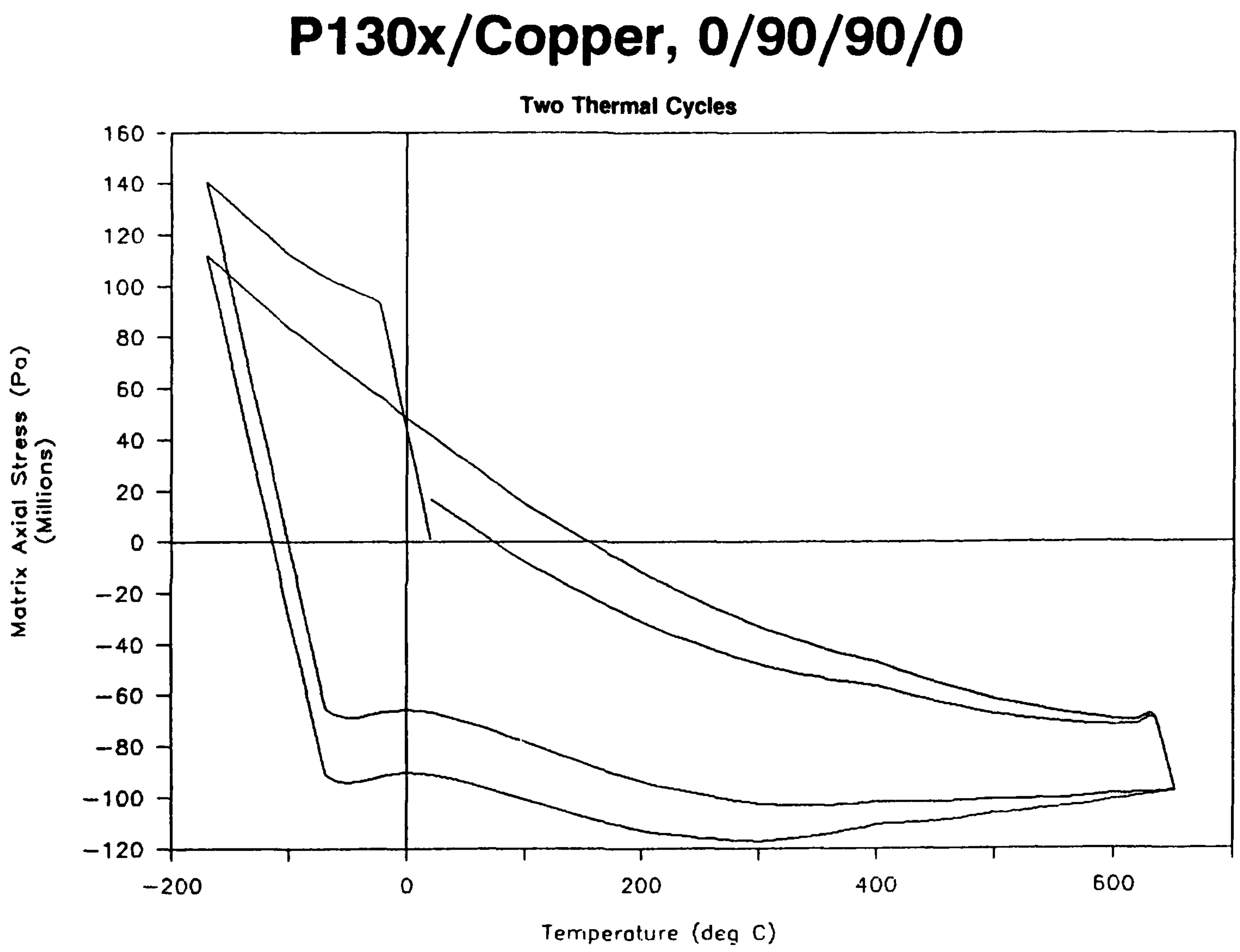

Figure 22. Matrix Axial Stress vs. Temperature.

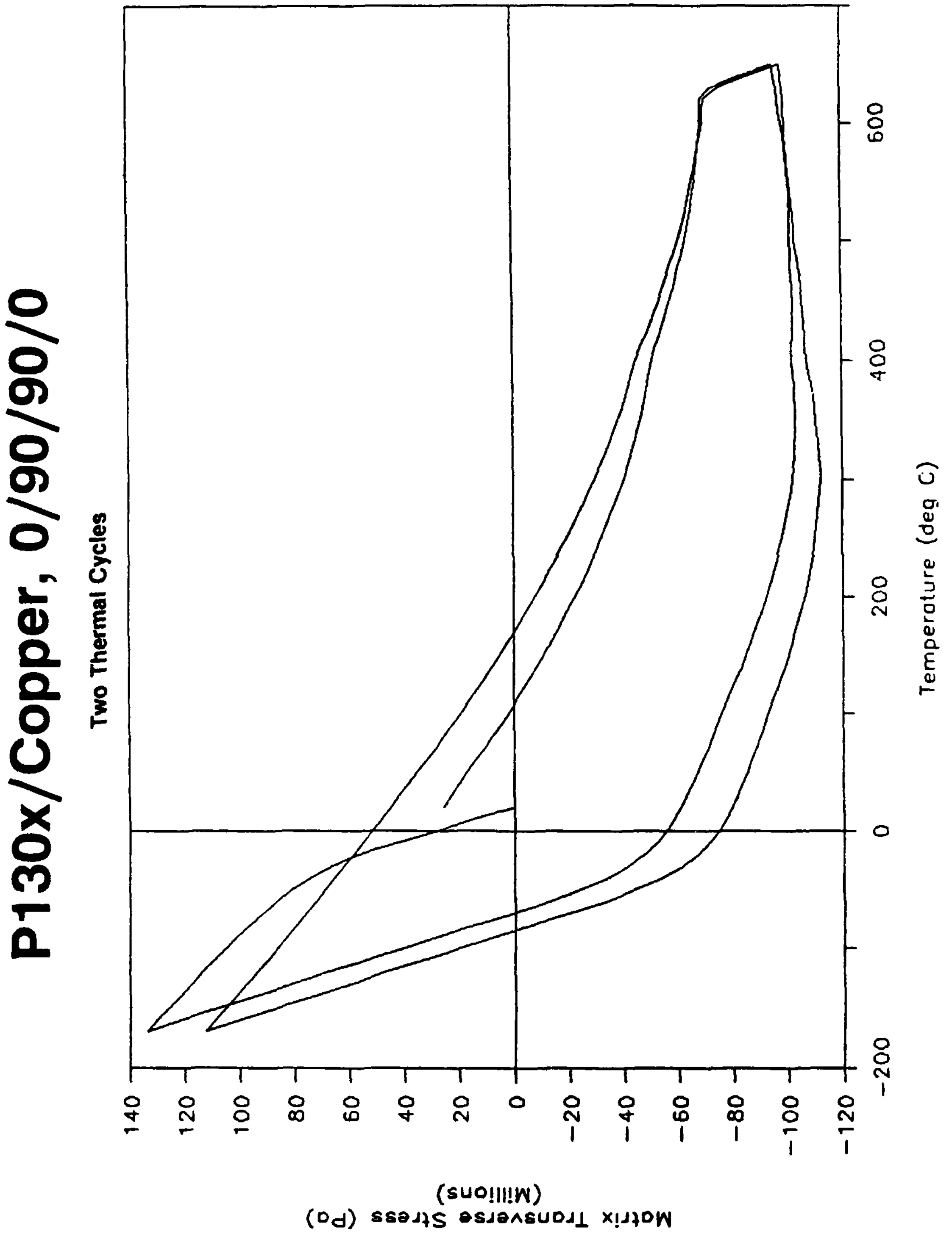

Figure 23. Matrix Transverse Stress vs. Temperature.

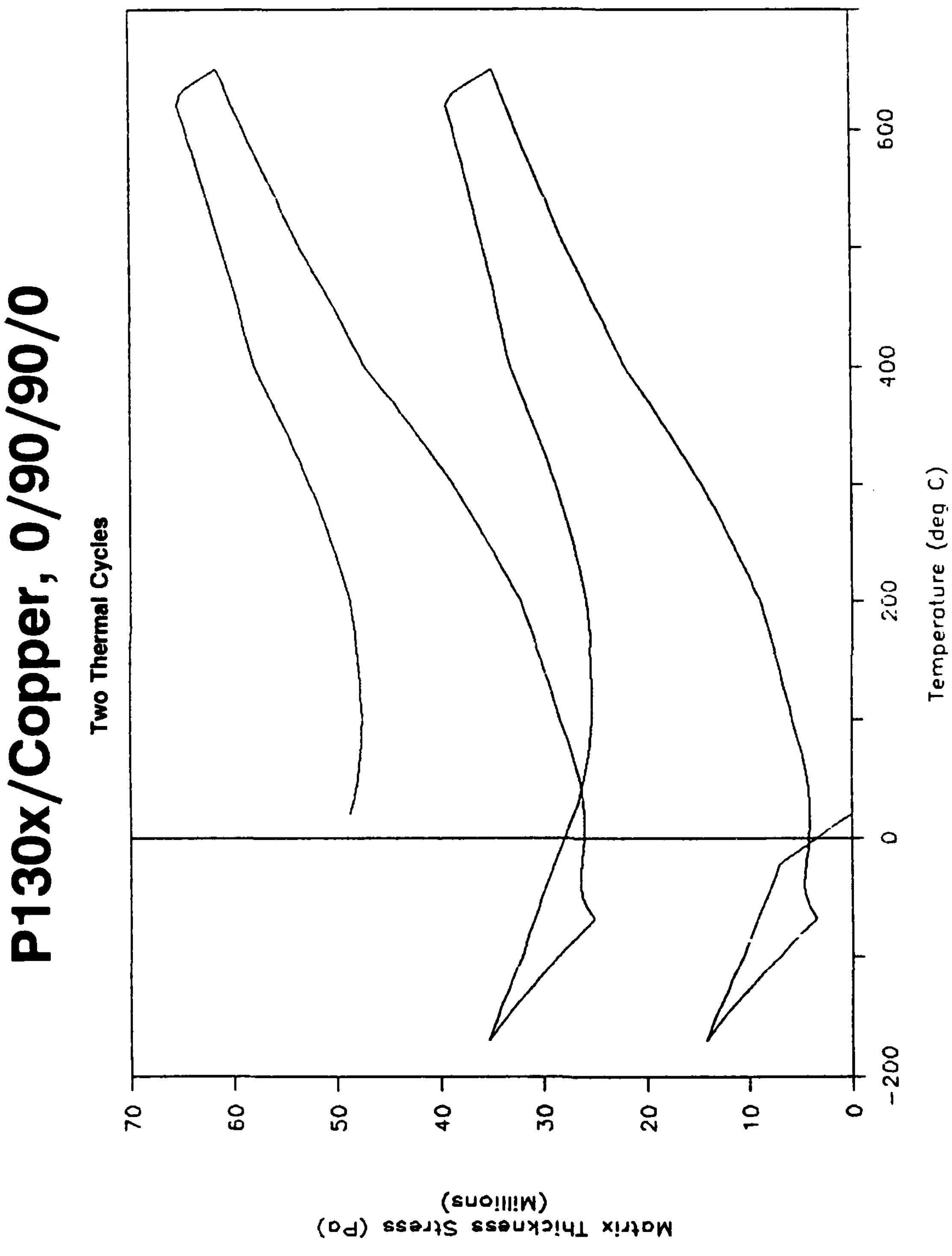

Figure 24. Matrix Thickness Stress vs. Temperature.

CONCLUSIONS

In this work a thermoplasticity model was formulated for the purpose of examining the mechanical and thermal behavior of MMC. The theoretical model was applied to the analyses of materials that are currently being proposed for use on advanced aerospace vehicles. The applications demonstrate the usefulness of the theory in predicting and interpreting basic material response. Also, the analysis data can be quickly changed to parametrically and inexpensively assess other designs.

For the P130x/copper material the analysis predicts that thermal cycling will lead to substantial plastic straining and hysteresis. Also, depending upon the construction, the hysteresis loops can ratchet under successive thermal loadings. The effect of the residual processing stresses was seen to be an upward or downward shifting of the response curves.

REFERENCES

1. Dvorak, G.J., Rao, M.S.M., and Tarn, J.Q., "Yielding in Unidirectional Composites Under External Loads and Temperature Changes," Journal of Composite Materials, Vol. 7, April 1973, pp. 194-216.

2. Adams, D.F., "Inelastic Analysis of a Unidirectional Composite Subjected to Transverse Normal Loading," Journal of Composite Materials, Vol. 4, July 1970, pp. 310-328.

3. Lin, T.H., Salinas, D., and Ito, Y.M., "Elastic-Plastic Analysis of Unidirectional Composites," Journal of Composite Materials, Vol. 6, January 1972, pp. 48-60.

4. Huang, W.C., "Plastic Behavior of Some Composite Materials," Journal of Composite Materials, Vol. 5, July 1971, pp. 320-338.

5. Dvorak, G.J., and Bahei-El-Din, Y.A., "Plasticity Analysis of Fibrous Composites," ASME Journal of Applied Mechanics, Vol. 49, June 1982, pp. 327-335.

6. Bahei-El-Din, Y.A., and Dvorak, G.J., "Plasticity Analysis of Laminated Composite Plates," ASME Journal of Applied Mechanics, Vol. 49, December 1982, pp. 740-746.

7. Kural, M.H., and Min, B.K., "The Effects of Matrix Plasticity on the Thermal Deformation of Continuous Fiber Graphite/Metal Composites," Journal of Composite Materials, Vol. 18, November 1984, pp. 519-535.

8. Foye, R.L., "Theoretical Post-Yielding Behavior of Composite Laminates Part II-Inelastic Micromechanics," Journal of Composite Materials, Vol. 7, July 1973, pp. 310-319.

9. Aboudi, J., and Benveniste, Y., "Constitutive Relations for Fiber Reinforced Inelastic Laminated Plates," ASME Journal of Applied Mechanics, Vol. 51, March 1984, pp. 107-113.

10. Buesking, K., "Nonlinear Unidirectional Metal Matrix Composite Behavior," DoD/NASA Annual Mechanics of Composites Review, October 1984, pp. 222-230.

11. Hashin, Z., "Theory of Fiber Reinforced Materials," NASA CR-1974, March 1972.

12. Hashin, Z., "Analysis of Properties of Fiber Composites with Anisotropic Constituents," ASME Journal of Applied Mechanics, Vol. 46, No. 3, September 1979, pp. 543-550.

13. Barrett, D.J., and Buesking, K.W., "Temperature Dependent Nonlinear Metal Matrix Laminate Behavior," NASA CR-4016, September 1986.

	No. of Copies
Sparta, Inc. Attn: Dr. K. Cheverton 4520 Executive Drive, Suite 210 San Diego, CA 92121-3020	1
Tuskegee University Attn: Vascar G. Harris, Dean School of Engineering and Architecture Tuskegee, AL 36088	1
Teledyne Ryan Aeronautical Company Attn: Mr. J. Hill 2701 N. Harbor Dr., MS 340H, Dept. 194 P.O. Box 80311 San Diego, CA 92138-9012	1
Villanova University Attn: Dr. P.V. McLaughlin Department of Mechanical Engineering Villanova, PA 19085	1
Virginia Polytechnic Institute Attn: Dr. K. Reifsnider Materials Response Group Blacksburg, VA 24061	1
University of Wyoming Attn: Dr. Donald Adams Professor of Mechanical Engineering Composite Material Research Group P.O. Box 3295 Laramie, WY 82071	1
NAVAIRDEVCEN Code 8131	2
NAVAIRDEVCEN Code 6043	25

	No. of Copies
Lockheed-Missile & Space Co. Attn: Mr. J.A. Bailie - Dept. 81-12 Bldg. 154 P.O. Box 504 1111 Lockheed Way Sunnyvale, CA 94088	1
LTV Aerospace and Defense Co. Vought Missiles and Advanced Programs Division Attn: Mr. R. Knight - MS-TH-83 P.O. Box 65003 Dallas, TX 75265-0003	1
Massachusetts Institute of Technology Attn: Dr. P.A. Lagace Dept. of Aeronautics and Astronautics Technology Laboratory for Advanced Composites 77 Massachusetts Avenue Cambridge, MA 02139	1
McDonnell Douglas Corporation McDonnell Aircraft Company Attn: Dr. Michael E. Renieri MS 370 Dept. 337, Bldg. 66 P.O. Box 516 St. Louis, MO 63166	1
University of Oklahoma Attn: Dr. C.W. Bert School of Aeronautics, Mechanical, Nuclear Engineering Norman, OK 73019	1
Pennsylvania State University Attn: Dr. T. Hahn Dept. Engineering Science & Mechanics 227 Hammond Building University Park, PA 16802	1
Purdue University Attn: Dr. C.T. Sun School of Aeronautics & Astronautics West Lafayette, IN 47907	1
Rockwell International Attn: Mr. M. Schweiger Columbus, OH 43216	1

	No. of Copies
General Dynamics Corporation Fort Worth Division Attn: Composite Structures Eng. Dept. P.O. Box 748 Fort Worth, TX 76101	1
General Electric Co. Space Systems Division Attn: Mr. A. Garber, MS M4018/BL100 P.O. Box 8555 Philadelphia, PA 19101	1
General Electric Co. Attn: Mr. C Zweben - MS M4018/BL 100 P.O. Box 8555 Philadelphia, PA 19101	1
Hercules Aerospace Division Attn: Mr. D. Hug P.O. Box 210 Rocket Center, WV 26726	1
HITCO Attn: Mr. N. Myers 1600 West 135th Street Gardena, CA 90249	1
Lehigh University Attn: Dr. G.C. Sih Institute of Fracture and Solid Mechanics Bethlehem, PA 18015	1
Lockheed Aeronautical Systems Company Attn: Mr. A.M. James Advanced Structures Technology Dept. Dept. 76-23, Bldg. 63, Plt. A-1 P.O. Box 551 Burbank, CA 91520	1
Lockheed-Georgia Co. Attn: Technical Information Dept. 72-34, Zone 26 Marietta, GA 30063	1

	No. of Copies
University of Delaware Attn: Dr. R.B. Pipes Mechanics & Aerospace Eng. Dept. Evans Hall Newark, DE 19711	1
University o' Delaware Attn: Dr. J.R. Vinson Mechanics & Aerospace Eng. Dept. Evans Hall Newark, DE 19711	1
University of Delaware Attn: Dr. D. Wilkins Mechanics & Aerospace Eng. Dept Evans Hall Newark, DE 19711	1
Department of Transportation Attn: Dr. Pin Tong, DTS 76, TSC Kendall Square Cambridge, MA 02142	1
Drexel University Attn: Dr. P.C. Chou Mechanical Engineering Dept. 32nd and Chestnut Street Philadelphia, PA 19104	1
Drexel University Attn: Dr. A.S.D. Wang Mechanical Engineering Dept. 32nd and Chestnut Street Philadelphia, PA 19104	1
Drexel University Attn: Dr. Frank Ko Fibrous Materials Research Lab 32nd and Chestnut Street Philadelphia, PA 19104	1
E.I. DuPont Company Attn: Mr. V.L. Bertarelli Chestnut Run Location, CR701 Wilmington, DE 19898	1

DISTRIBUTION LIST (Continued)
NADC-90004-60

	No. of Copies
Federal Aviation Administration Attn: L. Neri, Code ACT-330 Technical Center Atlantic City, NJ 08405	1
Administrator, Defense Technical Information Center Bldg. #5, Cameron Station Alexandria, VA 22314	2
Alcoa Defense Systems Corp. Attn: Mr. D. Myers 16761 Via delCampo Court San Diego, CA 92127	1
Anamet Laboratories, Inc. Attn: Dr. Rocky R. Arnold 3400 Industrial Way San Carlos, CA 94077	1
AVCO Attn: Mr. William F. Grant Speciality Materials Division 2 Industrial Avenue Lowell, MA 01851	1
Battelle Memorial Institute Metals and Ceramics Information Center 505 King Avenue Columbus, OH 43201	1
Bell Aerospace Company Attn: Mr. F.M. Anthony, Zone S-69 P.O. Box 1 Buffalo, NY 14240	1
University of California Attn: Professor Lawrence Rehfield Department of Mechanical Engineering Davis, CA 95616	1
University of Dayton Research Institute Attn: Dr. J. Gallagher 300 College Park Avenue Dayton, OH 45469	1

	No. of Copies
Administrator, National Aeronautics and Space Adm. Attn: Airframes Branch, FS 120 Washington, DC 20546	1
Administrator, National Aeronautics and Space Adm. Langley Research Center Attn: C.E. Harris, MS 188E Hampton, VA 23365-5225	1
Administrator, National Aeronautics and Space Adm. Langley Research Center Attn: J. Starnes, MS 190 Hampton, VA 23365-5225	1
Administrator, National Aeronautics and Space Adm. Langley Research Center Attn: Dr. M. Mikulus, MS 188A Hampton, VA 23365-5225	1
Administrator, National Aeronautics and Space Adm. George C. Marshall Space Flight Center Attn: R. Schwinghamer, S&E-ASTN-M Huntsville, AL 35812	1
Administrator, National Aeronautics and Space Adm. Lewis Research Center Attn: Dr. C. Chamis, MS 49-6 21000 Brookpark Rd. Cleveland, OH 44135	1
Administrator, National Aeronautics and Space Adm. Lewis Research Center Attn: M. Hershberg, MS 49-6 21000 Brookpark Rd. Cleveland, OH 44135	1
Administrator, National Aeronautics and Space Adm. Langley Research Center Attn: Mr. W.T. Freeman, Mail Code 243 Hampton, VA 23365-5225	1
Federal Aviation Administration Attn: Mr. J. R. Soderquist, AW 103 800 Independence Avenue, SW Washington, DC 20591	1

	No. of Copies
Commanding Officer, Wright Research and Development Center Attn: MLBM/Mr. M. Knight Wright Patterson Air Force Base, OH 45433-6533	1
Commanding Officer, Wright Research and Development Center Attn: MLBM/Dr. J. Whitney Wright Patterson Air Force Base, OH 45433-6533	1
Commanding Officer, Wright Research and Development Center Attn: MLSE/J. Reinhart Wright Patterson Air Force Base, OH 45433-6533	1
Commanding Officer, Wright Research and Development Center Attn: MLSE/F. Fecheck Wright Patterson Air Force Base, OH 45433-6533	1
Commanding Officer, U.S. Army Aviation Applied Technology Directorate Attn: G. McAllister USARTL, (AVRADCOM) Ft. Eustis, VA 23604-5418	1
Commanding Officer, U.S. Army Material & Mechanical Research Center Attn: D. Oplinger, SLCMT-MS Watertown, MA 02172-0001	1
Commanding Officer, U.S. Army R&T Laboratory (AVRADCOM) Attn: F. Immen, DAVDL-AS-MS 207-5 Ames Research Center Moffet Field, CA 94035	1
Commanding Officer, Picatinny Arsenal PLASTEC Attn: H. Pebly Dover, NJ 07801	1
Commanding Officer, Picatinny Arsenal PLASTEC Attn: Librarian, Code DRDAR-SCM-0 Bldg. 351N Dover, NJ 07801	1
Headquarters National Aeronautics and Space Adm. Attn: Dr. D. Mulville OAST-RM Washington, DC 20546	1

DISTRIBUTION LIST (Continued)
NADC-90004-60

	No. of Copies
Commander, David Taylor Research Center Attn: H. Edelstein, Code 2870 Annapolis, MD 21401	1
Commander, Naval Surface Weapons Center Attn: Dr. J. Goff - R-34 White Oak Laboratory Silver Spring, MD 20910	1
Commander, Naval Surface Weapons Center Attn: Dr. J.M. Augl 10901 New Hampshire Avenue Silver Spring, MD 20903-5000	1
Department of the Air Force Attn: Dr. M. Salkind Building 410 Bolling Air Force Base Washington, DC 20331	1
Department of the Air Force Attn: Dr. J. Amos Building 410 Bolling Air Force Base Washington, DC 20331	1
Commanding Officer, Wright Research and Development Center Attn: FIBEC/Dr. G. Sendeckyj Wright Patterson Air Force Base, OH 45433-6553	1
Commanding Officer, Wright Research and Development Center Attn: FIBA/L. Kelly Wright Patterson Air Force Base, OH 45433-6553	1
Commanding Officer, Wright Research and Development Center Attn: FIBA/W. Goesch Wright Patterson Air Force Base, OH 45433-6553	1
Commanding Officer, Wright Research and Development Center Attn: FIBCA/C. Ramsey Wright Patterson Air Force Base, OH 45433-6553	1
Commanding Officer, Wright Research and Development Center Attn: FIBR/H.F. Wolfe Wright Patterson Air Force Base, OH 45433-6553	1

	No. of Copies
Commander, Naval Air Systems Command Attn: T. Momiyama, AIR-931 Washington, DC 20361-9300	1
Commander, Naval Air Systems Command Attn: G. Seidel, AIR-931B Washington, DC 20361-9300	1
Commander, Naval Sea Systems Command Attn: C. Zannis, Sea 05R Washington, DC 20362	1
Commander, U.S. Naval Postgraduate School Attn: Professor R. Ball, Code 67BP Monterey, CA 93940	1
Commander, U.S. Naval Postgraduate School Attn: Dr. E. Robert Wood (Code 67) Monterey, CA 93940	1
Commander, U.S. Naval Postgraduate School Attn: Professor M.H. Bank, Code 67BP Monterey, CA 93943	1
Commander, U.S. Naval Postgraduate School Attn: Professor K. Challenger Monterey, CA 93943	1
Commander, United States Naval Academy Attn: Mechanical Engr. Department Annapolis, MD 21402	1
Commander, David Taylor Research Center Attn: A. Macander, Code 1720 Bethesda, MD 20084	1
Commander, David Taylor Research Center Attn: E.T. Camponeschi, Code 2844 Annapolis, MD 21402	1
Commander, David Taylor Research Center Attn: R. Crane, Code 2844 Annapolis, MD 21402	1
Commander, David Taylor Research Center Attn: Lori Wall, Code 17202 Bethesda, MD 20084-5000	1